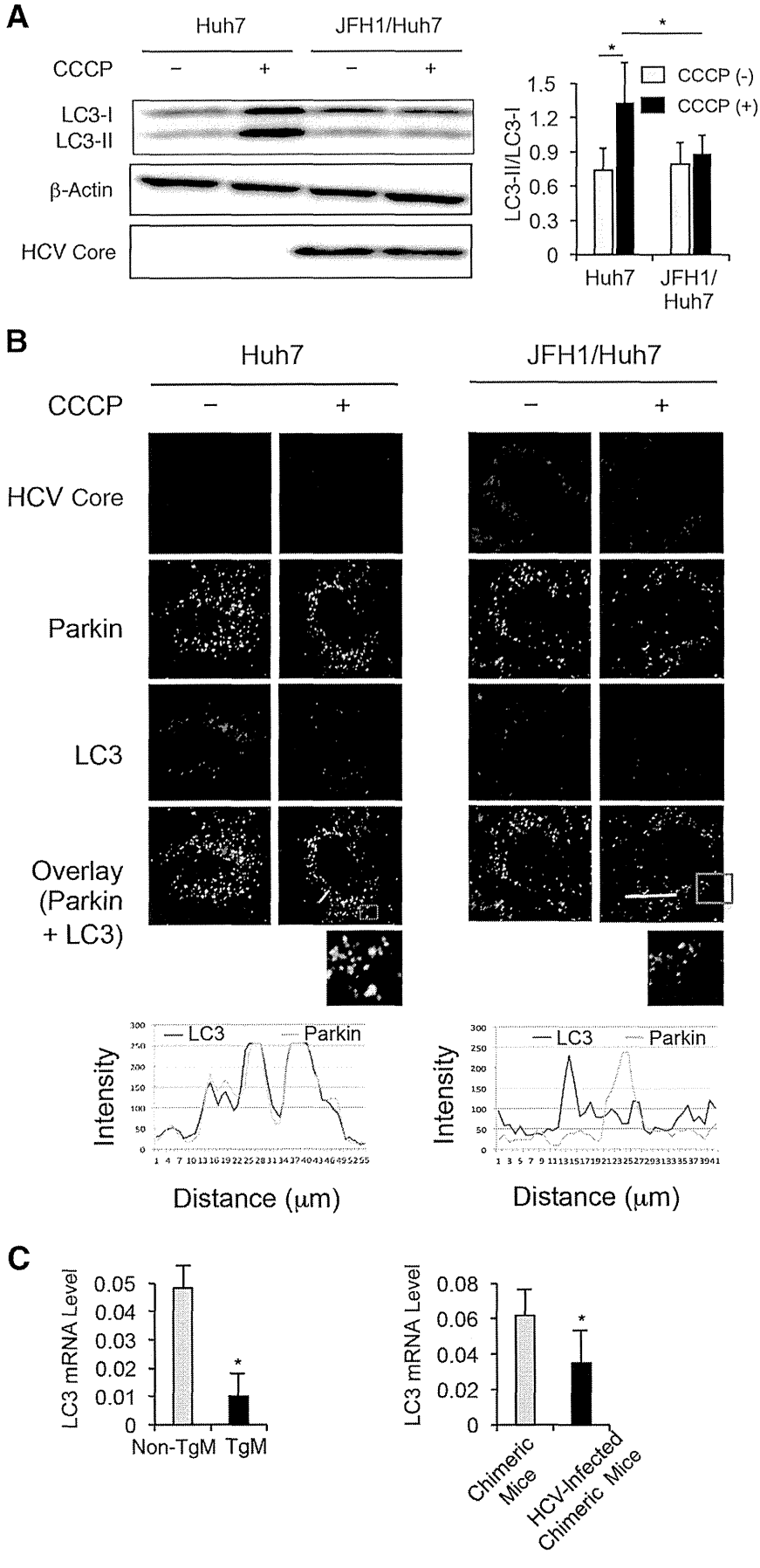

Figure 7 Effect of HCV infection on LC3-II expression and colocalization of Parkin with LC3 after carbonyl cyanide *m*-chlorophenylhydrazone (CCCP) treatment. **A:** Immunoblots for LC3-I and LC3-II using whole cell lysates of Huh7 and JFH1-Huh7 cells before and after CCCP treatment ($n = 5$). **B:** Immunofluorescence staining for Parkin (green) and LC3 (red) in Huh7 and JFH1-Huh7 cells before and after a 1-hour CCCP treatment. **Boxed areas** are enlarged below. Endogenous Parkin that colocalizes with LC3 (yellow spots). Line scans indicate the colocalization of Parkin with LC3 and correlate to the white lines in the images. **C:** The expression of LC3 mRNA in the liver from non-transgenic (non-TgM) and TgM mice ($n = 5$) and from chimeric mice without or with HCV infection ($n = 5$). The expression level of LC3 mRNA was normalized to GAPDH. $^*P < 0.05$.

mitochondria, was significantly reduced in JFH1-Huh7 cells compared with Huh7 cells (Figure 6F). Therefore, HCV infection clearly suppressed mitophagosome formation.

In agreement with suppressed mitophagosome formation, the LC3-II/I ratio was significantly lower after CCCP treatment in JFH1-Huh7 cells compared with Huh7 cells (Figure 7A), although the LC3-II/I ratio itself increased after CCCP treatment regardless of HCV infection. LC3 has been shown to be present in both complete autophagosomes and elongating isolation membranes that contain mitochondria ubiquitinated by Parkin. The present results indicate that Parkin colocalized with LC3 after CCCP treatment in Huh7 cells, whereas colocalization of Parkin and LC3 was significantly reduced in JFH1-Huh7 cells (Figure 7B). *In vivo*, FL-N/35-transgenic mice and HCV-infected chimeric mice also showed significantly reduced expression levels of LC3 mRNA in the liver compared with the control mice (Figure 7C), in agreement with reduced expression of Parkin in the mitochondrial fraction. These results may seem to be inconsistent with increased protein level of LC3-II after CCCP treatment *in vitro*. However, the lower LC3-II/I ratio after CCCP treatment in HCV-infected cells than in noninfected cells may reflect reduced expression levels of LC3 mRNA in FL-N/35-transgenic mice and HCV-infected chimeric mice. Further studies are required to clarify the mechanisms.

Several previous studies have proposed that autophagosome accumulation is enhanced on HCV infection and in HCV replicon cell lines.[34–38] Our findings of a decreased LC3-II/I ratio in JFH1-Huh7 cells, FL-N/35-transgenic mice, and HCV-infected chimeric mice seemingly contradict these previous reports. To clarify whether the decrease in LC3-II/I ratio observed in the present study indicated that macroautophagy (generally referred to as autophagy) or mitophagy was inhibited, we investigated LC3-II/I ratio in JFH1-Huh7 and Huh7 cells using Earle's balanced salt solution (EBSS) as a macroautophagy inducer (via amino acid starvation).[39] Interestingly, JFH1-Huh7 cells showed significantly increased LC3-II/I ratio compared with Huh7 cells after incubation with EBSS for 1 hour (Figure 8A), suggesting that HCV infection promoted autophagy under macroautophagy-inducible conditions. In agreement with increased LC3-II/I ratio, electron microscopy revealed that the number of autophagosomes was significantly greater after EBSS treatment in JFH1-Huh7 cells than in Huh7 cells (Figure 8B). Taken together with these results, the decrease in LC3-II/I ratio observed after CCCP treatment in JFH1-Huh7 cells likely represents a consequence of mitophagy inhibition, but not autophagy inhibition by HCV infection.

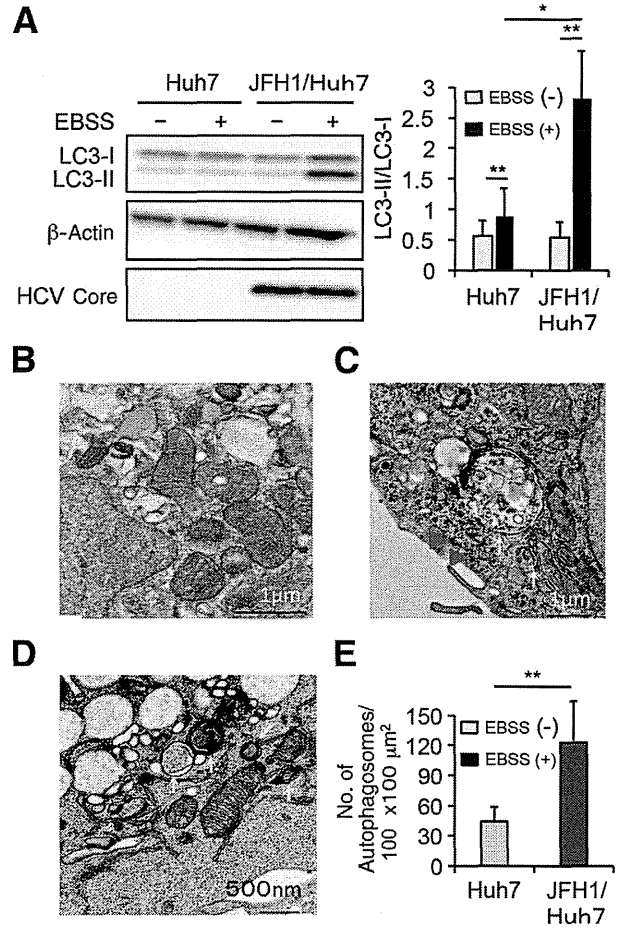

Figure 8 Effect of HCV infection on LC3-II expression and autophagosome formation after culture with Earle's balanced salt solution (EBSS). **A:** Immunoblots for LC3-II using Huh7 and JFH1-Huh7 cells before (−) and after (+) culture with EBSS ($n = 6$). The LC3-II and LC3-I expression level was normalized to β-actin. Electron microscopy of Huh7 (**B**) and JFH1-Huh7 (**C** and **D**) cells after EBSS treatment. The **arrows** indicate autophagosomes; **arrowheads**, HCV core protein. **E:** The number of autophagosomes per 100 × 100 μm² was calculated for five randomly selected views. $^{*}P < 0.05$, $^{**}P < 0.01$.

Suppression of Autophagic Degradation

The autophagic adaptor p62 can both aggregate ubiquitinated proteins by polymerizing with other p62 molecules and recruit ubiquitinated cargo into mitophagosomes by binding to LC3-II.[13] Therefore, p62 accumulation can be attributed to a deficit in autophagic degradation activity. After a 1- or 2-hour CCCP treatment, there was a smaller decrease in p62 in JFH1-Huh7 cells compared with Huh7 cells (Figure 9A). *In vivo*, FL-N/35-transgenic mice and HCV-infected chimeric mice also showed p62 accumulation in the liver compared with the control mice (Figure 9B). These results suggest that the degradation of damaged mitochondria was suppressed in the presence of HCV infection.

Finally, we assessed the change in VDAC1 content after CCCP treatment to obtain additional evidence as to whether mitophagy itself was suppressed by HCV infection. After a 2-hour CCCP treatment, a decrease in cellular content of VDAC1 was significantly smaller in JFH1-Huh7 cells than in Huh7 cells (Figure 9C). We also found that CCCP-induced increase in ROS production was greater in

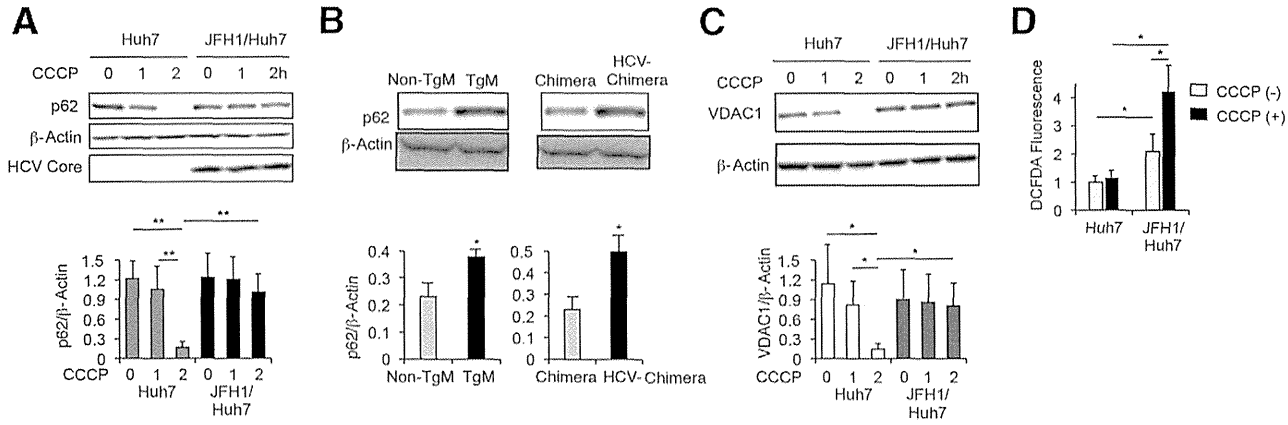

Figure 9 Effect of HCV infection on cellular p62 and VDAC1 expression after carbonyl cyanide *m*-chlorophenylhydrazone (CCCP) treatment and reactive oxygen species (ROS) production. **A:** Immunoblots for p62 using whole cell lysates of Huh7 and JFH1-Huh7 cells before and after a 1- and a 2-hour CCCP treatment ($n = 5$). **B:** Immunoblots for p62 using the liver from non-transgenic (non-TgM) and TgM ($n = 5$) mice and from chimeric mice without or with HCV infection ($n = 5$). The p62 expression level was normalized to β-actin. **C:** Immunoblots for VDAC1 using whole cell lysates of Huh7 and JFH1-Huh7 cells before and after a 1- and a 2-hour CCCP treatment ($n = 5$). The VDAC1 expression level was normalized to β-actin. **D:** Changes in cellular ROS production after a 1-hour CCCP treatment in Huh7 and JFH1-Huh7 cells ($n = 5$). $^{*}P < 0.05$, $^{**}P < 0.01$.

JFH1-Huh7 cells than in Huh7 cells (Figure 8D). These results were consistent with a previous study that showed an essential role of mitophagy in reducing mitochondrial ROS production[40] and, therefore, may reflect the suppressed mitophagy in the presence of HCV infection.

Discussion

Mitophagy may likely be induced in HCV-JFH1–infected cells in the context of mitochondrial depolarization, and in transgenic mice expressing the HCV polyprotein or in HCV-infected chimeric mice, both of which showed the decreased mitochondrial GSH content. Our results suggest that the HCV core protein inhibits mitophagy during HCV infection and that the molecular mechanisms by which this suppression occurs include the interaction of the HCV core protein with Parkin and the inhibition of Parkin translocation to the mitochondria. This inhibition leads to the failure of mitochondrial ubiquitination, mitophagosome formation, and autophagic degradation (Figure 10). Because Parkin 1 to 215 contains one of the critical amino acids required for mitochondrial localization, the specific interaction of Parkin 1 to 215 with the HCV core protein strongly suggests that the core protein represses mitophagy by inhibiting Parkin translocation to the mitochondria. We know that PINK1 accumulates in the mitochondria and phosphorylates Parkin after CCCP treatment and that the suppression of the mitochondrial Parkin signal occurs by blocking PINK1 via siRNA. Therefore, we could exclude the possibility that PINK1 plays a role in suppressing the recruitment of Parkin to the mitochondria. To our knowledge, this is the first report to demonstrate a suppressive effect of a viral protein on mitophagy via an interaction with Parkin. Interestingly, silencing Parkin via siRNA inhibited HCV core expression, which was consistent with the results of a recent study.[28] These results suggest that HCV potentially uses Parkin for its replication through the interaction between the HCV core protein and Parkin. Parkin may be post-transcriptionally involved in HCV replication, because Parkin silencing did not affect HCV core mRNA levels.

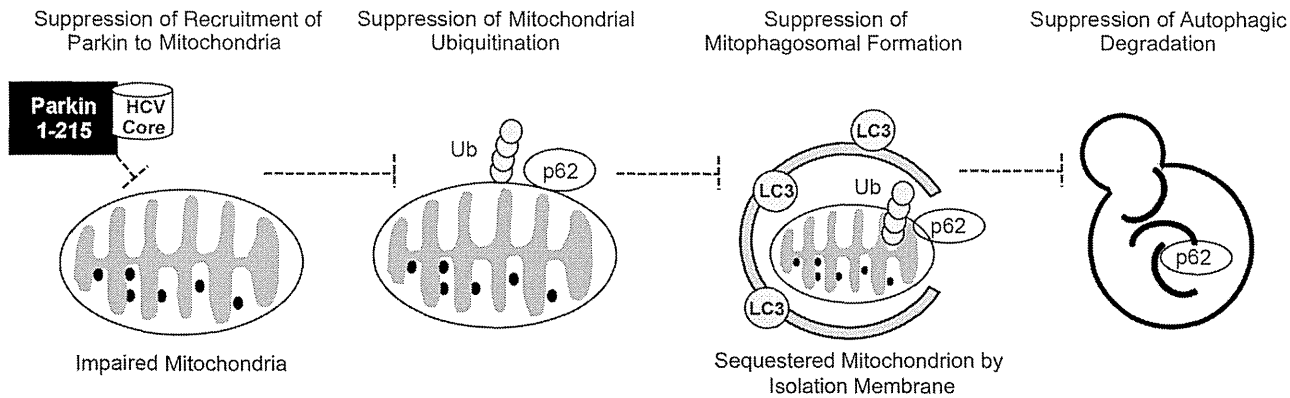

Figure 10 A schematic diagram depicting the mechanisms underlying mitophagy suppression by the HCV core protein. The HCV core protein interacts with the Parkin N-terminal fragment containing the RINGO domain (designated Parkin 1 to 215) and inhibits Parkin translocation to the mitochondria, which leads to the failure of mitochondrial ubiquitination, autophagosome formation, and autophagic degradation. Ub, ubiquitin.

Further studies are required to clarify the mechanisms underlying this speculation.

Two types of autophagy have been identified: nonselective and selective. For nonselective autophagy related to HCV infection, previous studies have reported the enhanced accumulation of autophagosomes without any effect on autophagic protein degradation,[33] the requirement of LC3 for efficient HCV replication,[34] and the occurrence of HCV RNA replication on autophagosomal membranes.[36] Mitophagy is selective and is induced by mitochondrial membrane depolarization, followed by Parkin recruitment to the mitochondria.[9–15] Herein, mitophagosome accumulation was suppressed because of mitophagy inhibition, whereas HCV infection enhanced the expression of LC3-II and autophagosome accumulation under nonselective autophagy-inducible conditions. Therefore, the present results are consistent with the previously characterized HCV-induced nonselective autophagic response.[34,35,38] However, a recent report has shown that HCV induces the mitochondrial translocation of Parkin and subsequent mitophagy,[28] which contrasts with the present results, except for the inhibitory effect of Parkin silencing on HCV replication. One of the significant differences in the method between the two studies was the presence or absence of CCCP treatment. Whether HCV-induced mitophagy was preceded by mitochondrial depolarization was unknown because $\Delta\Psi$ was not measured in the previous report of HCV-induced mitophagy.[28] However, we need to be careful that the mitochondrial depolarization by CCCP treatment is not a pathophysiological condition observed in HCV infection and that CCCP causes the depolarization of the entire mitochondrial network.[41] It is currently unknown whether CCCP treatment caused paradoxical results on mitophagy in HCV-infected cells between our study and a previous one.[28] Although suppressed mitophagy was also found in FL-N/35-transgenic mice and HCV-infected chimeric mice without any treatment, these mice may not be simply compared with HCV-JFH1–infected cells in terms of extremely low levels of viral proteins in FL-N/35-transgenic mice or spontaneous oxidized mitochondrial glutathione in both mice. Another difference between two studies was postinfection time from infection to assessment of mitophagy in HCV-JFH1–infected cells (21 versus 3 days). However, further studies are required to clarify whether postinfection time of HCV-JFH1–infected cells affects the interaction of HCV with Parkin. Oxidative stress and/or hepatocellular mitochondrial alterations are present in chronic hepatitis C to a greater degree than in other inflammatory liver diseases,[1,6] and mitophagy is important for maintaining mitochondrial quality by eliminating damaged mitochondria. Therefore, our results that the HCV core protein suppresses mitophagy appear reasonable in the context of what is known about the pathophysiological characteristics of chronic hepatitis C.

HCV-induced mitochondrial injury, ROS production, and subsequent oxidative stress contribute to HCC development in FL-N/35-transgenic mice that receive modest iron supplementation.[8] The relatively long period (12 months) required for HCC development suggests that mitochondrial injury, as a source of oxidative stress, must continue for a prolonged period. Mitochondrial DNA mutations are also relevant to HCC development in patients with chronic HCV infections.[42] Indeed, mitophagy plays an essential role in reducing mitochondrial ROS production and mitochondrial DNA mutations in yeast[40] and eliminating oxidative damaged mitochondria.[43] In addition to the directly induced generation of ROS by HCV proteins, the suppression of mitophagy by the HCV core protein has the potential to generate an additional long-lasting ROS burden and may offset or overwhelm the physiological antioxidative activity in mitochondria. Therefore, the suppressive effect of the HCV core protein on mitophagy may be an important mechanism of HCV-induced hepatocarcinogenesis.

In conclusion, results indicate that HCV core protein suppresses mitophagy by inhibiting Parkin translocation to the mitochondria via a direct interaction with Parkin in the context of mitochondrial depolarization. These findings have implications for the amplification and sustainability of mitochondria-induced oxidative stress observed in patients with HCV-related chronic liver disease and an increased risk of hepatocarcinogenesis.

Acknowledgments

We thank Dr. Stanley M. Lemon for the transgenic mice, Dr. Takaji Wakita for the JFH1 clone, and Hikari Hara for technical assistance.

References

1. Farinati F, Cardin R, De Maria N, Della Libera G, Marafin C, Lecis E, Burra P, Floreani A, Cecchetto A, Naccarato R: Iron storage, lipid peroxidation and glutathione turnover in chronic anti-HCV positive hepatitis. J Hepatol 1995, 22:449–456
2. Valgimigli M, Valgimigli L, Trere D, Gaiani S, Pedulli GF, Gramantieri L, Bolondi L: Oxidative stress EPR measurement in human liver by radical-probe technique: correlation with etiology, histology and cell proliferation. Free Radic Res 2002, 36:939–948
3. Okuda M, Li K, Beard MR, Showalter LA, Scholle F, Lemon SM, Weinman SA: Mitochondrial injury, oxidative stress, and antioxidant gene expression are induced by hepatitis C virus core protein. Gastroenterology 2002, 122:366–375
4. Moriya K, Nakagawa K, Santa T, Shintani Y, Fujie H, Miyoshi H, Tsutsumi T, Miyazawa T, Ishibashi K, Horie T, Imai K, Todoroki T, Kimura S, Koike K: Oxidative stress in the absence of inflammation in a mouse model for hepatitis C virus-associated hepatocarcinogenesis. Cancer Res 2001, 61:4365–4370
5. Korenaga M, Wang T, Li Y, Showalter LA, Chan T, Sun J, Weinman SA: Hepatitis C virus core protein inhibits mitochondrial electron transport and increases reactive oxygen species (ROS) production. J Biol Chem 2005, 280:37481–37488
6. Barbaro G, Di Lorenzo G, Asti A, Ribersani M, Belloni G, Grisorio B, Filice G, Barbarini G: Hepatocellular mitochondrial alterations in patients with chronic hepatitis C: ultrastructural and biochemical findings. Am J Gastroenterol 1999, 94:2198–2205

7. Nishina S, Hino K, Korenaga M, Vecchi C, Pietrangelo A, Mizukami Y, Furutani T, Sakai A, Okuda M, Hidaka I, Okita K, Sakaida I: Hepatitis C virus-induced reactive oxygen species raise hepatic iron level in mice by reducing hepcidin transcription. Gastroenterology 2008, 134:226–238
8. Furutani T, Hino K, Okuda M, Gondo T, Nishina S, Kitase A, Korenaga M, Xiao SY, Weinman SA, Lemon SM, Sakaida I, Okita K: Hepatic iron overload induces hepatocellular carcinoma in transgenic mice expressing the hepatitis C virus polyprotein. Gastroenterology 2006, 130:2087–2098
9. Kim I, Rodriguez-Enriquez S, Lemasters JJ: Selective degradation of mitochondria by mitophagy. Arch Biochem Biophys 2007, 462:245–253
10. Elmore SP, Qian T, Grissom S, Lemasters JJ: The mitochondrial permeability transition initiates autophagy in rat hepatocytes. FASEB J 2001, 15:2286–2287
11. Matsuda N, Sato S, Shiba K, Okatsu K, Saisho K, Gautier CA, Sou YS, Saiki S, Kawajiri S, Sato F, Kimura M, Komatsu M, Hattori N, Tanaka K: PINK1 stabilized by mitochondrial depolarization recruits Parkin to damaged mitochondria and activates latent Parkin for mitophagy. J Cell Biol 2010, 189:211–221
12. Narendra DP, Jin SM, Tanaka A, Suen DF, Gautier CA, Shen J, Cookson MR, Youle RJ: PINK1 is selectively stabilized on impaired mitochondria to activate Parkin. PLoS Biol 2010, 8:e1000298
13. Geisler S, Holmström KM, Skujat D, Fiesel FC, Rothfuss OC, Kahle PJ, Springer W: PINK1/Parkin-mediated mitophagy is dependent on VDAC1 and p62/SQSTM1. Nat Cell Biol 2010, 12:119–131
14. Vives-Bauza C, Zhou C, Huang Y, Cui M, de Vries RL, Kim J, May J, Tocilescu MA, Liu W, Ko HS, Magrane J, Moore DJ, Dawson VL, Grailhe R, Dawson TM, Li C, Tieu K, Przedborski S: PINK1-dependent recruitment of Parkin to mitochondria in mitophagy. Proc Natl Acad Sci USA 2010, 107:378–383
15. Narendra D, Tanaka A, Suen DF, Youle RJ: Parkin is recruited selectively to impaired mitochondria and promotes their autophagy. J Cell Biol 2008, 183:795–803
16. Chan NC, Salazar AM, Pham AH, Sweredoski MJ, Kolawa NJ, Graham RL, Hess S, Chan DC: Broad activation of the ubiquitin-proteasome system by Parkin is critical for mitophagy. Hum Mol Genet 2011, 20:1726–1737
17. Gegg ME, Cooper JM, Chau KY, Rojo M, Schapira AH, Taanman JW: Mitofusin 1 and mitofusin 2 are ubiquitinated in a PINK1/parkin-dependent manner upon induction of mitophagy. Hum Mol Genet 2010, 19:4861–4870
18. Chen D, Gao F, Li B, Wang H, Xu Y, Zhu C, Wang G: Parkin mono-ubiquitinates Bcl-2 and regulates autophagy. J Biol Chem 2010, 285: 38214–38223
19. Narendra D, Kane LA, Hauser DN, Fearnley IM, Youle RJ: p62/SQSTM1 is required for Parkin-induced mitochondrial clustering but not mitophagy: VDAC1 is dispensable for both. Autophagy 2010, 6:1090–1106
20. Itakura E, Kishi-Itakura C, Koyama-Honda I, Mizushima N: Structures containing Atg9A and the ULK1 complex independently target depolarized mitochondria at initial stages of Parkin-mediated mitophagy. J Cell Sci 2012, 125:1488–1499
21. Okatsu K, Saisho K, Shimanuki M, Nakada K, Shitara H, Sou YS, Kimura M, Sato S, Hattori N, Komatsu M, Tanaka K, Matsuda N: p62/SQSTM1 cooperates with Parkin for perinuclear clustering of depolarized mitochondria. Genes Cells 2010, 15:887–900
22. Wakita T, Pietschmann T, Kato T, Date T, Miyamoto M, Zhao Z, Murthy K, Habermann A, Kräusslich HG, Mizokami M, Bartenschlager R, Liang TJ: Production of infectious hepatitis C virus in tissue culture from a cloned viral genome. Nat Med 2005, 11:791–796
23. Li K, Prow T, Lemon SM, Beard MR: Cellular response to conditional expression of hepatitis C virus core protein in Huh7 cultured human hepatoma cells. Hepatology 2002, 35:1237–1246
24. Lerat H, Honda M, Beard MR, Loesch K, Sun J, Yang Y, Okuda M, Gosert R, Xiao SY, Weinman SA, Lemon SM: Steatosis and liver cancer in transgenic mice expressing the structural and nonstructural proteins of hepatitis C virus. Gastroenterology 2002, 122:352–365
25. Tateno C, Yoshizane Y, Saito N, Kataoka M, Utoh R, Yamasaki C, Tachibana A, Soeno Y, Asahina K, Hino H, Asahara T, Yokoi T, Furukawa T, Yoshizato K: Near completely humanized liver in mice shows human-type metabolic responses to drugs. Am J Pathol 2004, 165:901–912
26. Kimura T, Imamura M, Hiraga N, Hatakeyama T, Miki D, Noguchi C, Mori N, Tsuge M, Takahashi S, Fujimoto Y, Iwao E, Ochi H, Abe H, Maekawa T, Arataki K, Tateno C, Yoshizato K, Wakita T, Okamoto T, Matsuura Y, Chayama K: Establishment of an infectious genotype 1b hepatitis C virus clone in human hepatocyte chimeric mice. J Gen Virol 2008, 89:2108–2113
27. Ando M, Korenaga M, Hino K, Ikeda M, Kato N, Nishina S, Hidaka I, Sakaida I: Mitochondrial electron transport inhibition in full genomic hepatitis C replicon cells is restored by reducing viral replication. Liver Int 2008, 28:1158–1166
28. Kim SJ, Syed GH, Siddiqui A: Hepatitis C virus induces the mitochondrial translocation of Parkin and subsequent mitophagy. PLoS Pathog 2013, 9:e1003285
29. Toida K, Kosaka K, Aika Y, Kosaka T: Chemically defined neuron groups and their subpopulations in the glomerular layer of the rat main olfactory bulb. IV: intraglomerular synapses of tyrosine hydroxylase-immunoreactive neurons. Neuroscience 2000, 101:11–17
30. Ikeda M, Sugiyama K, Mizutani T, Tanaka T, Tanaka K, Sekihara H, Shimotohno K, Kato N: Human hepatocyte clonal cell lines that support persistent replication of hepatitis C virus. Virus Res 1998, 56: 157–167
31. Zhang GJ, Liu HW, Yang L, Zhong YG, Zheng YZ: Influence of membrane physical state on the lysosomal proton permeability. J Membr Biol 2000, 175:53–62
32. Sharpe MA, Wrigglesworth JM, Loewen J, Nicholls P: Small pH gradients inhibit cytochrome c oxidase: implications for H+ entry to the binuclear center. Biochem Biophys Res Commun 1995, 216: 931–938
33. Hristova VA, Beasley SA, Rylett RJ, Shaw GS: Identification of a novel Zn2+-binding domain in the autosomal recessive juvenile Parkinson-related E3 ligase parkin. J Biol Chem 2009, 284:14978–14986
34. Sir D, Chen WL, Choi J, Wakita T, Yen TS, Ou JH: Induction of incomplete autophagic response by hepatitis C virus via the unfolded protein response. Hepatology 2008, 48:1054–1061
35. Dreux M, Gastaminza P, Wieland SF, Chisari FV: The autophagy machinery is required to initiate hepatitis C virus replication. Proc Natl Acad Sci U S A 2009, 106:14046–14051
36. Ke PY, Chen SS: Activation of the unfolded protein response and autophagy after hepatitis C virus infection suppresses innate antiviral immunity in vitro. J Clin Invest 2011, 121:37–56
37. Sir D, Kuo CF, Tian Y, Liu HM, Huang EJ, Jung JU, Machida K, Ou JH: Replication of hepatitis C virus RNA on autophagosomal membranes. J Biol Chem 2012, 287:18036–18043
38. Shrivastava S, Bhanja Chowdhury J, Steele R, Ray R, Ray RB: Hepatitis C virus upregulates Beclin1 for induction of autophagy and activates mTOR signaling. J Virol 2012, 86:8705–8712
39. Munafo DB, Colombo MI: A novel assay to study autophagy: regulation of autophagosome vacuole size by amino acid deprivation. J Cell Sci 2001, 114:3619–3629
40. Kurihara Y, Kanki T, Aoki Y, Hirota Y, Saigusa T, Uchiumi T, Kang D: Mitophagy plays an essential role in reducing mitochondrial production of reactive oxygen species and mutation of mitochondrial DNA by maintaining mitochondrial quantity and quality in yeast. J Biol Chem 2012, 287:3265–3272
41. Wang Y, Nartiss Y, Steipe B, McQibban GA, Kim PK: ROS-induced mitochondrial depolarization initiates PARK2/PARKIN-dependent mitochondrial degradation by autophagy. Autophagy 2012, 8:1462–1476
42. Nishikawa M, Nishiguchi S, Shiomi S, Tamori A, Koh N, Takeda T, Kubo S, Hirohashi K, Kinoshita H, Sato E, Inoue M: Somatic mutation of mitochondrial DNA in cancerous and noncancerous liver tissue in individuals with hepatocellular carcinoma. Cancer Res 2001, 61:1843–1845
43. Venditti P, Di Stefano L, Di Meo S: Mitochondrial metabolism of reactive oxygen species. Mitochondrion 2013, 13:71–82

Bioorganic & Medicinal Chemistry Letters 24 (2014) 4276–4280

Contents lists available at ScienceDirect

Bioorganic & Medicinal Chemistry Letters

journal homepage: www.elsevier.com/locate/bmcl

Synthesis and inhibitory activity on hepatitis C virus RNA replication of 4-(1,1,1,3,3,3-hexafluoro-2-hydroxy-2-propyl)aniline analogs

Kenji Matsuno [a,*], Youki Ueda [b], Miwa Fukuda [a], Kenji Onoda [a], Minoru Waki [a], Masanori Ikeda [b], Nobuyuki Kato [b], Hiroyuki Miyachi [a,*]

[a] Medicinal and Bioorganic Chemistry, Graduate School of Medicine, Dentistry and Pharmaceutical Sciences, Okayama University, 1-1-1 Tsushima-naka, Kita-ku, Okayama 700-8530, Japan
[b] Department of Tumor Virology, Graduate School of Medicine, Dentistry and Pharmaceutical Sciences, Okayama University, 2-5-1 Shikata-cho, Kita-ku, Okayama 700-8558, Japan

ARTICLE INFO

Article history:
Received 11 June 2014
Revised 3 July 2014
Accepted 8 July 2014
Available online 15 July 2014

Keywords:
Hepatitis C virus
HCV RNA replication
Anti-HCV agent
Full genome length
ORL8

ABSTRACT

Using our recently developed assay system for full-genome-length hepatitis C virus (HCV) RNA replication in human hepatoma-derived Li23 cells (ORL8), we identified 4-(1,1,1,3,3,3-hexafluoro-2-hydroxy-2-propyl)aniline analog **1a** as a novel HCV inhibitor. Structural modifications of **1a** provided a series of sulfonamides **7** with much more potent HCV RNA replication-inhibitory activity than ribavirin. Compound **7a** showed an additive anti-HCV effect in combination with standard anti-HCV therapy (IFN-α plus ribavirin). Since **7a** generated reactive oxygen species (ROS) in the ORL8 system and its anti-HCV activity was blocked by vitamin E, its anti-HCV activity may be mediated at least in part by ROS.

Hepatitis C virus (HCV), an enveloped, single-stranded RNA virus, is a major cause of human hepatitis. It is estimated that ca. 150 million people worldwide are chronically infected with this virus, and more than 350,000 people die every year from hepatitis C-related liver disease.[1] Most infections become persistent and about 60% of cases progress to chronic liver disease, which in turn can lead to cirrhosis, hepatocellular carcinoma, and liver failure. Currently, no anti-HCV vaccine is available, and the standard treatment for chronic hepatitis C consists of pegylated interferon (IFN)-α in combination with the classical anti-HCV agent ribavirin. Recently, telaprevir, boceprevir and simeprevir, which are members of a new class of HCV NS3-4A serine-protease inhibitors, have been approved for hepatitis C treatment as combination therapy with pegylated IFN-α and ribavirin for patients with HCV genotype ***1a or 1b. Although these new therapies have increased cure rates for both previously untreated people and prior non-responders, there are still non-responders to these treatments. Also, serious adverse reactions such as skin reaction may require discontinuation of the combination therapy. Thus, new anti-HCV agents are still required, not only to extend the coverage of current therapy, but also because of the high mutation and replication rates of HCV.

The HCV genome consists of 9,600 bases encoding three structural and seven non-structural proteins.[2] So far, drug discovery programs for anti-HCV agents have focused on NS3 protease and NS5B polymerase as targets to block HCV replication. Conventionally, HCV replication assay has generally been conducted with sub-genomic HCV replicon systems encoding minimum sequences for autonomous HCV replication, that is, HCV replicase proteins NS3 to NS5B, with firefly luciferase as the reporter gene.[3] However, we recently developed new screening systems to identify HCV inhibitors, namely a reporter gene assay system with *Renilla* luciferase for replication of genome-length HCV RNA in human hepatoma-derived HuH-7 cells (OR6)[4] and in human hepatoma-derived Li23 cells (ORL8).[5] Figure 1 shows a schematic representation of the gene organization in the genome-length HCV RNA in ORL8. These full-genomic systems are considered to be superior to the conventional sub-genomic systems, and are suitable for use in chemical-biological approaches to detect different types of HCV inhibitors due to the different genetic backgrounds of HuH-7 and Li23 cells.[6] By use of these assays, we identified *N*-{4-(1,1,1,3,3,3-hexafluoro-2-hydroxy-2-propyl)phenyl}-*N*-methylbenzamide (**1a**) as a novel HCV inhibitor (Fig. 2). Compound **1a** is a much more potent inhibitor of HCV RNA replication (EC_{50} 0.32 μM) than ribavirin (EC_{50} 8.7 μM). Interestingly, the ORL8 assay system

* Corresponding authors.
E-mail address: matz@pharm.okayama-u.ac.jp (K. Matsuno).

http://dx.doi.org/10.1016/j.bmcl.2014.07.019
0960-894X/

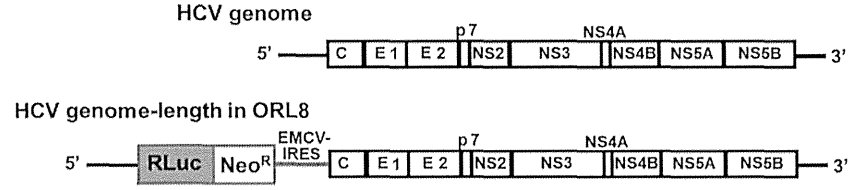

Figure 1. Schematic illustration of the gene organization in HCV genome-length in ORL8. *Abbreviations:* RLuc, *Renilla* luciferase gene; NeoR, neomycin phosphotransferase; EMCV-IRES, encephalomyocarditis virus internal ribosomal entry site.

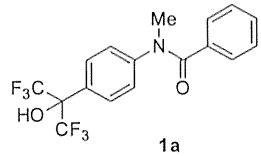

1a

EC_{50} = 0.32μM (ORL8)
EC_{50} > 20μM (OR6)

Figure 2. Structure of **1a** and HCV RNA replication-inhibitory activity in the ORL8 and OR6 assay systems.

was more sensitive to **1a** than the OR6 system. Herein, we describe the synthesis of **1a** and its derivatives modified at both phenyl rings, as well as at the hexafluoroisopropanol group and the amide moiety. The structure–activity relationship of these compounds for HCV RNA replication was examined, and the mechanism of action is discussed.

The synthetic procedures are outlined in Scheme 1. Briefly, condensation of (1,1,1,3,3,3-hexafluoro-2-hydroxy-2-propyl)-aniline **3a** with acyl chloride, sulfonyl chloride or isocyanate provided amides (**1a–1u**), sulfonamides (**7a–7i**) or urea (**8**), respectively. Compound **3a** was obtained as the major product by alkylation of aniline **2** with hexafluoroacetone trihydrate under acidic conditions.[7] Compound **3b** was also formed as a minor product, so the regioisomer of the hexafluoroisopropanol group (**4**) was synthesized from **3b** by benzoylation. Incorporation of substituents on phenyl rings and phenyl ring replacement were achieved by using the corresponding commercially available aniline **2**, acyl chloride or sulfonyl chloride. 1,1,1,3,3,3-Hexafluoro-2-(2-hydroxyethoxy)propyl analog **6** was synthesized from THP-protected **5**, which was obtained by alkylation of **1a** with commercially available 2-(2-bromoethoxy)tetrahydro-2*H*-pyran. The aminomethylene analog **9** was synthesized by direct incorporation of a hexafluoroisopropanol moiety into *N*-benzyl-*N*-methylaniline.

All synthetic analogs were assayed for anti-HCV RNA replication activity in the ORL8 system and EC_{50} values were determined (Tables 1 and 2). The values of 50% cytotoxic concentration (CC_{50}) for Li23 cells were determined by conventional WST-1 assay, and the values of selectivity index (SI), that is CC_{50}/EC_{50}, were calculated. All assays were conducted in triplicate.

The results of modifications at both phenyl rings and at the hexafluoroisopropanol group are summarized in Table 1. The incorporation of Me on the left phenyl ring (**1b**, **1c**) reduced anti-HCV RNA replication activity, and the 3-Me analog was completely inactive. Methylation of the right phenyl ring (**1d–1f**) also decreased anti-HCV activity. Among compounds with replacement of the right phenyl ring (**1g–1q**), alkyl analogs showed moderate activity. Extension of the alkyl chain increased the activity (**1g–1i**) and the cyclohexyl analog **1j** was as potent as the parent **1a**, with an adequate SI value. Bulky 1-adamantyl analog **1k** was a

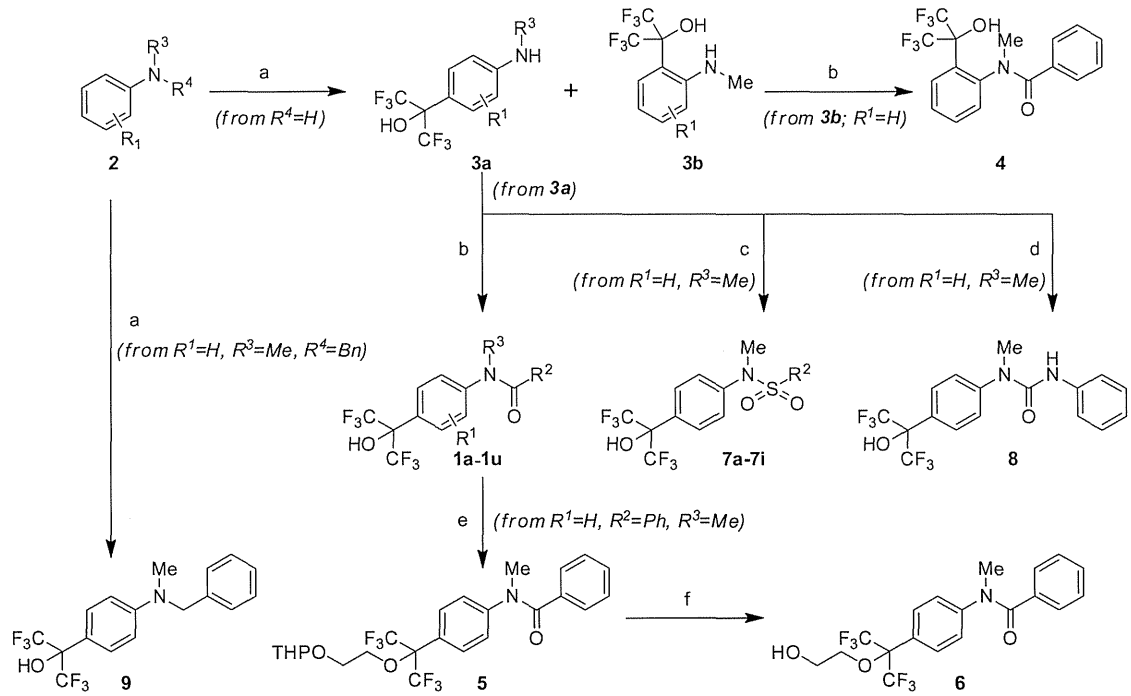

Scheme 1. Synthesis of 4-(1,1,1,3,3,3-hexafluoro-2-hydroxy-2-propyl)aniline analogs. Reagents and conditions: (a) hexafluoro-acetone trihydrate, *p*TsOH hydrate, toluene, reflux, 71–93%; (b) R^2-COCl, Et_3N, toluene or $CHCl_3$, 22–93%; (c) R^2-SO_2Cl, Et_3N, CH_2Cl_2, quant.; (d) PhNCO, toluene, quant.; (e) $THPOCH_2CH_2Br$, Cs_2CO_3, DMF, 79%; (f) *p*TsOH hydrate, *i*PrOH, H_2O, quant.

Table 1
Values of HCV RNA replication-inhibitory activity, cytotoxicity and safety index of **1a–1q**, **4** and **6** in ORL8 assay

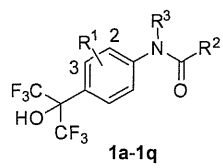
1a-1q

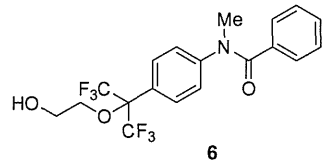
6

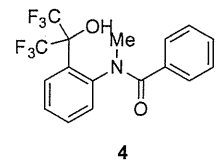
4

Compd no	R^1	R^2	R^3	EC_{50} (μM)	CC_{50} (μM)	SI[a]
1a	H	Ph	Me	0.32	65	203
1b	2-Me	Ph	Me	1.7	9.0	5.3
1c	3-Me	Ph	Me	>100	87	ND[b]
1d	H	2-Me-Ph	Me	17	38	2.2
1e	H	3-Me-Ph	Me	5.8	20	3.4
1f	H	4-Me-Ph	Me	10	26	2.6
1g	H	Me	Me	14	40	2.9
1h	H	nPr	Me	3.8	>100	ND[b]
1i	H	nBu	Me	2.3	26	11
1j	H	cHex	Me	0.23	20	87
1k	H	1-Adamantyl	Me	1.0	17	17
1l	H	CH_2Ph	Me	>100	27	ND[b]
1m	H	2-pyridyl	Me	>100	>100	ND[b]
1n	H	3-pyridyl	Me	45	63	1.4
1o	H	4-pyridyl	Me	8.2	40	4.9
1p	H	2-thienyl	Me	2.6	33	13
1q	H	3-thienyl	Me	17	44	2.6
6				11	>20	ND[b]
4				>20	>20	ND[b]

[a] Selectivity index (CC_{50}/EC_{50}).
[b] Not determined.

Table 2
Values of HCV RNA replication-inhibitory activity, cytotoxicity and safety index of **1r–1u**, **7a–7i**, **8** and **9** in ORL8 assay

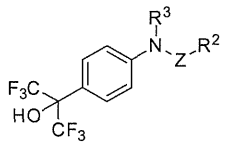
Z=CO (**1r-1u**)
Z=SO_2 (**7a-7i**)
Z=CONH (**8**)
Z=CH_2 (**9**)

Compd no	R^2	R^3	EC_{50} (μM)	CC_{50} (μM)	SI[a]
1r	Ph	H	4.1	12	2.9
1s	Ph	Et	0.78	19	24
1t	Ph	nPr	3.5	15	4.3
1u	Ph	Bn	2.9	7.5	2.6
7a	Ph	Me	0.19	16	84
7b	2-Cl-Ph	Me	0.17	15	88
7c	2-Br-Ph	Me	0.50	9.1	18
7d	2-Me-Ph	Me	0.36	12	33
7e	3-F-Ph	Me	0.36	19	53
7f	3-Me-Ph	Me	0.35	11	31
7g	4-Me-Ph	Me	0.44	15	34
7h	3-MeO-Ph	Me	2.1	13	6.2
7i	4-MeO-Ph	Me	1.4	7.9	5.6
8	Ph	Me	5.7	>20	ND[b]
9	Ph	Me	3.0	13	4.3

[a] Selectivity index (CC_{50}/EC_{50}).
[b] Not determined.

moderately active HCV inhibitor, while the benzyl analog **1l** was inactive. This result suggests the importance of the orientation of the hydrophobic moiety (vide infra). Suggestively, 2-pyridyl analog **1m**, whose hydrophilic N atom is located at the most proximal position to the amide moiety, was completely inactive. The conformation of the two aromatic rings could differ from those of other pyridyl analogs (**1n–1o**) at low pH values, such as that in endosomes of cells (vide infra).[8] Bioisosteric replacement of the phenyl ring with thiophene (**1p–1q**) decreased the activity.

As for hexafluoroisopropanol modifications, 2-hydroxyethoxy analog **6** was a weak HCV inhibitor. This result suggests that the acidity of OH might be important for anti-HCV activity (calculated pK_a[9] of OH group: 7.7 for **1a**, 14.4 for **6**, respectively). The position of the hexafluoroisopropanol group appears to be critical, since regioisomer **4** was inactive.

Inhibitory activities of the amide-modified analogs on HCV RNA replication are listed in Table 2. Among them, sulfonamide analog **7a** showed potent anti-HCV activity. In contrast to the amide series, substituents on the right phenyl ring (**7b–7g**) had little detrimental effect, except for OMe analogs (**7h–7i**), which showed >10-fold weaker activity and low SI values. Both deletion of the Me group on the amide moiety (**1r**) and extension of the alkyl group (**1s–1u**) decreased the anti-HCV activity. Insertion of NH (urea analog **8**) and carba replacement of the amide carbonyl (aminomethylene analog **9**) also reduced the anti-HCV activity by about 10-fold compared with **1a**. It is generally accepted that benzanilide takes *transoid* conformation, whereas *N*-methylated benzanilide uniquely takes *cisoid* conformation in aqueous solution.[10] We speculate that adequate proximity of the right phenyl ring (or hydrophobic group such as cHex) to the left phenyl ring, namely *cisoid* conformation of amide, is favorable for potent inhibition of HCV RNA replication. This would be consistent with the inactivity of the 2-pyridyl analog (**1m**), which would adopt *transoid* conformation at low pH.[8] Also, this is also supported by the following speculations; the moderate inhibitor urea **8** takes similar conformation of **1a**, namely *cisoid* (at –NMeCO–)-*transoid* (at –CONH–) conformation,[11] whereas the inactive benzyl analog **1l** might take complete cofacial conformation of the two phenyl ring due to the π–π stacking interaction.

Next, the effect of adding **7a** to current standard HCV therapy (IFN-α plus ribavirin) was evaluated (Fig. 3). In our ORL8 assay system, HCV RNA replication was dose-dependently reduced both by IFN-α alone and by IFN-α plus ribavirin. Addition of **7a** dose-dependently enhanced the inhibition of HCV RNA replication by these agents. Also, addition of **7a** to IFN-α plus ribavirin was more

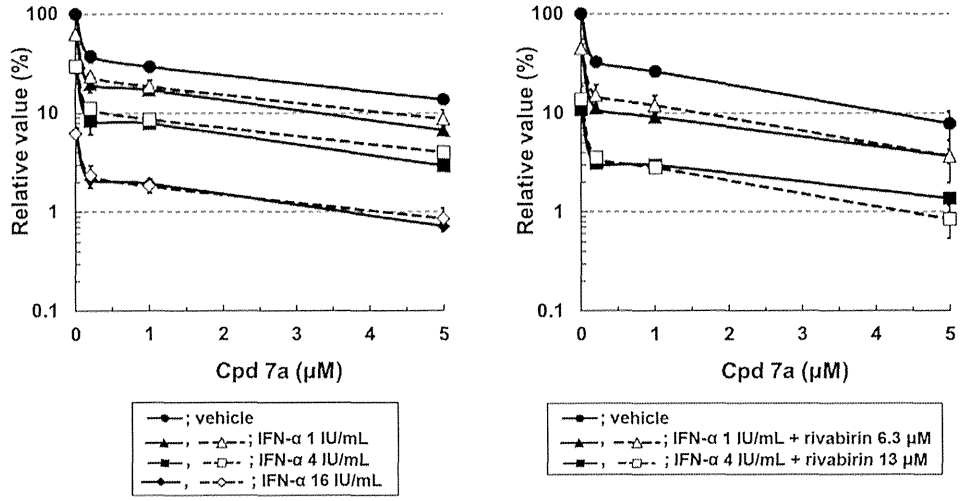

Figure 3. Additive effect of **7a** on HCV RNA replication in combination with IFN-α alone (left) and with IFN-α + ribavirin (right). (Left) circle: vehicle, triangle: IFN-α 1 IU/mL (IU: international unit), box: IFN-α 4 IU/mL), diamond: IFN-α 16 IU/mL. (Right) circle: vehicle, triangle: IFN-α 1 IU/mL + ribavirin 6.3 μM, box: IFN-α 4 IU/mL + ribavirin 13 μM. Open symbols in the broken lines show the values expected as an additive anti-HCV effect, and closed symbols in the solid lines show the values obtained by the ORL8 assay. Assays were conducted in triplicate.

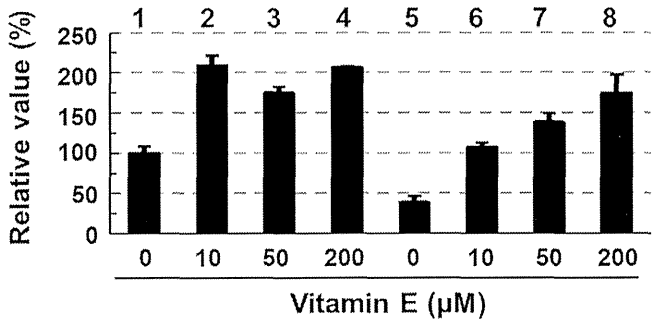

Figure 4. Effect of vitamin E on anti-HCV activity of **7a**. 1–4: in the absence of **7a**, 5–8: in the presence of 5 μM **7a** (60% inhibitory concentration for HCV RNA replication). Assays were conducted in triplicate.

effective than addition to IFN-α alone at the same concentration of IFN-α. These observations indicate that combination of **7a** with the current standard therapy might improve the cure rate of HCV infection.

Finally, the effect of vitamin E on the anti-HCV activity of **7a** was evaluated. As we previously reported, vitamin E strongly enhances HCV RNA replication.[12] Here, we examined the effect of vitamin E at various concentrations on HCV RNA replication in the presence of **7a** at the 60% inhibitory concentration level. As shown in Figure 4, vitamin E enhanced HCV RNA replication and dose-dependently blocked the anti-HCV activity of **7a**. We speculate that the 4-(1,1,1,3,3,3-hexafluoro-2-hydroxy-2-propyl)aniline analogs synthesized in this study have nuclear receptor-modulating activity, since structurally similar T0901317 is known to be a modulator of multiple nuclear receptors (NRs), including liver X receptor (LXR),[13] retinoic acid receptor-related orphan receptor gamma (RORγ)[14] and farnesoid X receptor (FXR).[15] Modulation of NRs produces reactive oxygen species (ROS) in various cells.[16,17] Indeed, **7a** dose-dependently produced ROS in the ORL8 assay system as determined by FACS analysis (data not shown). Therefore, we speculated that the mechanism of the anti-HCV activity of **7a** involves inhibition of HCV RNA replication by ROS produced via modulation of unknown NR(s). Indeed, scavenging of ROS by the antioxidant vitamin E blocked the anti-HCV activity of **7a**. Detailed studies on the mechanism of action of **7a** are ongoing.

In conclusion, *N*-{4-(1,1,1,3,3,3-hexafluoro-2-hydroxy-2-propyl)phenyl}-*N*-methylbenzamide (**1a**) was identified as a novel HCV inhibitor by use of our recently developed assay system for full-genome-length HCV RNA replication in Li23 cells (ORL8). Structural modifications of **1a** provided a series of sulfonamides **7** that showed potent inhibition of HCV RNA replication. Compound **7a** showed an additive anti-HCV effect in combination with standard HCV therapy (IFN-α plus ribavirin). The anti-HCV action of **7a** may be mediated by ROS production, since it was abrogated by vitamin E.

Acknowledgments

This work was supported by the Drug Discovery for Intractable Infectious Diseases Project, Graduate School of Medicine, Dentistry and Pharmaceutical Sciences, Okayama University from the Ministry of Education, Culture, Sports, Science and Technology (MEXT). The authors appreciate Mr. Yoshiaki Masuda of PharmaDesign Inc., Tokyo for the pK_a calculations. The authors thank the Division of Instrumental Analysis, Okayama University for the NMR measurements.

References and notes

1. World Health Organization fact sheet N°164 Hepatitis C (http://www.who.int/mediacentre/factsheets/fs164/en/) April 2014.
2. Bartenschlager, R.; Frese, M.; Pietschmann, T. *Adv. Virus Res.* **2004**, *63*, 71.
3. Lohmann, V.; Bartenschlager, R. *J. Med. Chem.* **2014**, *57*, 1627.
4. Ikeda, M.; Abe, K.; Dansako, H.; Nakamura, T.; Naka, K.; Kato, N. *Biochem. Biophys. Res. Commun.* **2005**, *329*, 1350.
5. Kato, N.; Mori, K.; Abe, K.; Dansako, H.; Kuroki, M.; Ariumi, Y.; Wakita, T.; Ikeda, M. *Virus Res.* **2009**, *146*, 41.
6. Mori, K.; Ikeda, M.; Ariumi, Y.; Kato, N. *Hepatol. Res.* **2010**, *40*, 1248.
7. Farah, B. S.; Gilbert, E. E.; Sibilia, J. P. *J. Org Chem.* **1965**, *30*, 998.
8. Okamoto, I.; Nabeta, M.; Minami, T.; Nakashima, A.; Morita, N.; Takeya, T.; Masu, H.; Azumaya, I.; Tamura, O. *Tetrahedron Lett.* **2007**, *48*, 573.
9. Calculated pK_a values were determined with ACD/Labs Percepta 2012 Release using the GALAS (Global, Adjusted Locally According to Similarity) algorithm.
10. Itai, A.; Toriumi, Y.; Tomioka, N.; Kagechika, H.; Azumaya, I.; Shudo, K. *Tetrahedron Lett.* **1989**, *30*, 6177.
11. Matsumura, M.; Tanatani, A.; Azumaya, I.; Masu, H.; Hashizume, D.; Kagechika, H.; Muranaka, A.; Uchiyama, M. *Chem. Commun.* **2013**, 2290.
12. Yano, M.; Ikeda, M.; Abe, K.; Dansako, H.; Ohkoshi, S.; Aoyagi, Y.; Kato, N. *Antimicrob. Agents Chemother.* **2007**, *51*, 2016.
13. Schultz, J. R.; Tu, H.; Luk, A.; Repa, J. J.; Medina, J. C.; Li, L.; Schwendner, S.; Wang, S.; Thoolen, M.; Mangelsdorf, D. J.; Lustig, K. D.; Shan, B. *Genes Dev.* **2000**, *14*, 2831.

14. Fauber, B. P.; Boenig, G. L.; Burton, B.; Eidenschenk, C.; Everett, C.; Gobbi, A.; Hymowitz, S. G.; Johnson, A. R.; Liimatta, M.; Lockey, P.; Norman, M.; Ouyang, W.; René, O.; Wong, H. *Bioorg. Med. Chem. Lett.* **2013**, *23*, 6604.
15. Houck, K. A.; Borchert, K. M.; Hepler, C. D.; Thomas, J. S.; Bramlett, K. S.; Michael, L. F.; Burris, T. P. *Mol. Gen. Metab.* **2004**, *83*, 184.
16. Fontaine, C.; Rigamonti, E.; Nohara, A.; Gervois, P.; Teissier, E.; Fruchart, J.-C.; Staels, B.; Chinetti-Gbaguidi, G. *Circ. Res.* **2007**, *101*, 40.
17. Raichur, S.; Lau, P.; Staels, B.; Muscat, G. E. O. *J. Mol. Endocrinol.* **2007**, *39*, 29.

Virology 462-463 (2014) 166-174

Contents lists available at ScienceDirect

Virology

journal homepage: www.elsevier.com/locate/yviro

Rab18 is required for viral assembly of hepatitis C virus through trafficking of the core protein to lipid droplets

Hiromichi Dansako [a], Hiroki Hiramoto [a], Masanori Ikeda [a], Takaji Wakita [b], Nobuyuki Kato [a,*]

[a] Department of Tumor Virology, Okayama University Graduate School of Medicine, Dentistry and Pharmaceutical Sciences, 2-5-1 Shikata-cho, Kita-ku, Okayama 700-8558, Japan
[b] Department of Virology II, National Institute of Infectious Disease, 1-23-1 Toyama, Shinjuku-ku, Tokyo 162-8640, Japan

ARTICLE INFO

Article history:
Received 14 February 2014
Returned to author for revisions
11 March 2014
Accepted 14 May 2014

Keywords:
Hepatitis C virus
Rab18
Viral assembly
Lipid droplet
Core protein
RNA replication

ABSTRACT

During persistent infection of HCV, the HCV core protein (HCV-JFH-1 strain of genotype 2a) is recruited to lipid droplets (LDs) for viral assembly, but the mechanism of recruitment of the HCV core protein is uncertain. Here, we demonstrated that one of the Ras-related small GTPases, Rab18, was required for trafficking of the core protein around LDs. The knockdown of Rab18 reduced intracellular and extracellular viral infectivity, but not intracellular viral replication in HCV-JFH-1-infected RSc cells (an HuH-7-derived cell line). Exogenous expression of Rab18 increased extracellular viral infectivity almost two-fold. Furthermore, Rab18 was co-localized with the core protein in HCV-JFH-1-infected RSc cells, and the knockdown of Rab18 blocked recruitment of the HCV-JFH-1 core protein to LDs. These results suggest that Rab18 has an important role in viral assembly through the trafficking of the core protein to LDs.

Introduction

Hepatitis C virus (HCV) is an enveloped positive single-stranded RNA virus belonging to the *Flaviviridae* family (Choo et al., 1989). The HCV genome encodes a large polyprotein precursor of approximately 3000 amino acid (aa) residues, which is cleaved co- and post-translationally into at least ten proteins in the following order: core, envelope 1 (E1), E2, p7, nonstructural protein 2 (NS2), NS3, NS4A, NS4B, NS5A, and NS5B (Kato, 2001). Persistent HCV infection in the liver causes chronic hepatitis, and then highly progresses to liver cirrhosis and hepatocellular carcinoma (Ohkoshi et al., 1990). Therefore, the elimination of HCV RNA by the anti-HCV reagents such as interferon is necessary to block the progression of liver diseases such as liver cirrhosis and hepatocellular carcinoma. To date, the HCV-JFH-1 strain (genotype 2a) has mainly been used to study the complete life cycle of HCV worldwide. In HCV-JFH-1-infected human hepatoma HuH-7 cells, viral replication intermediate, double-stranded RNA, is detected adjacent to the membranes of the endoplasmic reticulum (ER) (Targett-Adams et al., 2008). In addition, the HCV replication complex is formed on a detergent-resistant membrane (Shi et al., 2003). These results suggest that HCV RNA replication occurs on lipid rafts and the membranous web at the cytosolic side of the ER. Following viral replication, the HCV core protein matures through the translation of a large polyprotein precursor from HCV RNA and then the processing by signal peptide peptidase. The matured HCV-JFH-1 core protein has been shown to be trafficked to lipid droplets (LDs) for viral assembly (Miyanari et al., 2007).

LDs are important organelles for lipid metabolism. LDs are covered by a phospholipid monolayer, and accumulate excessive neutral lipids such as triglycerides. A proteomics analysis revealed that a number of host factors are associated with LDs (Brasaemle et al., 2004). These host factors are required for acquisition, storage, lipolysis, transport and/or release of lipids, respectively. The first of these LD-associated factors to be identified were members of the PAT family of proteins, including perilipin (PLIN), ADRP (adipose differentiation-related protein; also named adipophilin or PLIN2), and TIP47 (also named PLIN3). PLIN is expressed only in adipocytes and steroidogenic cells, whereas ADRP and TIP47 are expressed in various cell types. ADRP and TIP47 have similar sequences and three-dimensional structures (Hickenbottom et al., 2004), but their intracellular distributions in HuH-7 cells are different (Ohsaki et al., 2006). ADRP localizes exclusively to the surface of LDs in HuH-7 cells, whereas only some of total TIP47 localizes to the LD surface in this cell line. During viral assembly, the core protein is trafficked to ADRP on LDs (Counihan et al., 2011). ADRP is displaced from the surface of LDs to the cytoplasm by the core protein, and then subjected to degradation (Boulant et al., 2008). These displacements

* Corresponding author. Fax: +81 86 235 7392.
E-mail address: nkato@md.okayama-u.ac.jp (N. Kato).

http://dx.doi.org/10.1016/j.virol.2014.05.017
0042-6822/

of ADRP also cause the redistribution of LDs around the nucleus (Boulant et al., 2008). These observations imply that the core protein may increase the probability of an interaction between the sites of viral replication at the ER and viral assembly at the LDs. However, the precise mechanism of intracellular trafficking of the core protein to ADRP on LDs is still uncertain.

A family of Ras-related small GTPases plays an important role in the membrane trafficking between organelles such as the ER, Golgi, early/late endosomes, LDs, and so on (Hutagalung and Novick, 2011). One of the Ras-related small GTPases, Rab18, is required for membrane trafficking between the ER and Golgi (Dejgaard et al., 2008). On the other hand, Rab18 is an LD-associated protein, and the ectopic expression of Rab18 induces the close apposition of LDs to ER membranes through the reduction of ADRP (Ozeki et al., 2005). These observations imply that Rab18 may be required for membrane trafficking through the redistribution of LDs around the ER. Recently, Salloum et al. reported that Rab18 bound HCV-JFH-1 NS5A and may have promoted the interaction between sites of viral replication and LDs in HCV-Jc1-infected Huh7.5.1 cells (Salloum et al., 2013). However, HCV-Jc1 is an intragenotypic recombinant encoding core to NS2 from the HCV-J6 strain (genotype 2a) in the context of HCV-JFH-1, and does not exist in nature. In addition, although HCV-Jc1 was shown to be more robust in the release of viral particles than HCV-JFH-1, the HCV-J6 core protein did not associate with LDs (Shavinskaya et al., 2007). On the other hand, the HCV-JFH-1 core protein does associate with LDs, and LD-associated core proteins recruit HCV NS protein from the ER to LDs (Miyanari et al., 2007). These results imply that HCV-Jc1 may release viral particles via an intracellular organelle distinct from the LDs. Therefore, we hypothesized that Rab18 first trafficked the HCV-JFH-1 core protein and subsequently NS5A to LD. To prove this hypothesis, we examined the association of the HCV-JFH-1 core protein with LDs and the levels of viral assembly in Rab18-knockdown cells.

Here, we show that Rab18 is required for trafficking of the HCV-JFH-1 core protein to LDs and the subsequent assembly of HCV. Rab18 may be involved in the maturation of viral particles through membrane trafficking of the HCV-JFH-1 core protein from the sites of viral replication at the ER to viral assembly at the LDs in human hepatocytes.

Results

RSc cells show higher viral productivity than Huh7.5 cells

To date, human hepatoma HuH-7 cells have mainly been used to study the complete life cycle of HCV in studies worldwide. One of the sublines of HuH-7 cells, Huh7.5, is used in many laboratories for its high susceptibility to infection with the HCV-JFH-1 strain (genotype 2a). On the other hand, we have previously established several types of HCV RNA-replicating cells (genotype 1b, O strain), such as sO cells (Kato et al., 2003, sub-genomic HCV RNA), O cells (Ikeda et al., 2005, genome-length HCV RNA), and OR6 cells (Ikeda et al., 2006, genome-length HCV RNA-encoding renilla luciferase) derived from HuH-7 cells, and their "cured" cells (sOc (Kato et al., 2003), Oc (Ikeda et al., 2005), OR6c (Ikeda et al., 2006), respectively) by the elimination of HCV RNA (Fig. 1A). The cured cell lines have been reported to increase the permissiveness of HCV (Blight et al., 2002). We also previously reported that Oc cells showed higher permissiveness of HCV than sOc cells (Abe et al., 2007). RSc cells are one of our cured cell lines derive from OR6c cells, and have mainly been used to study the complete life cycle of HCV in our laboratory (Ariumi et al., 2007, 2008; Kato et al., 2009). However, we have no information on viral susceptibility of our cured cell lines to HCV-JFH-1 infection. To identify which of our cured cell lines would be most useful for the infection with HCV-JFH-1, we first compared the amounts of LDs by two methods, i.e., a confocal microscope and flow cytometry. The LDs were stained with BODIPY493/503 and observed under a confocal microscope. In our cured cells (sOc, Oc, OR6c, and RSc cells), the numbers rather than the sizes of LDs have increased compared to HuH-7 cells (Fig. 1B). In addition, the mean fluorescence intensity of BODIPY493/503-stained cells has increased by the enhancements of the numbers of LDs (Fig. 1C). These qualitative and quantitative analyses revealed that our cured cells (sOc, Oc, OR6c, and RSc cells) formed higher levels of LDs than HuH-7 and Huh7.5 cells (Fig. 1B and C). Interestingly, irrespective of the quantitative difference of LDs, the levels of viral replication at 72 h after the viral inoculation of HCV-JFH-1 were comparable between each of our cured cell lines and Huh7.5 cells, but not between each of the cured cell lines and HuH-7 cells (Fig. 1D). Moreover, the time-course analysis showed that the capacities of HCV RNA replication were almost comparable between RSc and Huh7.5 cells (Fig. 1E). These results suggest that the levels of HCV RNA replication do not depend on the amount of LDs. Next, to compare the levels of viral assembly and viral productivity between RSc and Huh7.5 cells, we examined the infectivity of the cell lysates (intracellular infectivity) and the supernatants (extracellular infectivity) derived from both lines of HCV-JFH-1-infected cells. The intracellular and extracellular infectivities of HCV-JFH-1-infected RSc cells were significantly higher than those of HCV-JFH-1-infected Huh7.5 cells (Fig. 1F). These results suggest that RSc cells possess higher viral productivity in response to infection with HCV-JFH-1 than Huh7.5 cells.

Rab18 is required for viral production, but not viral RNA replication

As the first step of viral assembly, the HCV-JFH-1 core protein displaces ADRP from the surface of LDs to the cytoplasm (Boulant et al., 2008; Counihan et al., 2011). In the present study, we tried to clarify how the core protein is trafficked to LDs by using RSc and Huh7.5 cells. It has been reported that Rab18, one of the Ras-related small GTPase family members, induces the close apposition of LDs to ER membranes through the reduction of ADRP (Ozeki et al., 2005). Based on these previous findings, we hypothesized that Rab18 is required for trafficking of the HCV-JFH-1 core protein to LDs. To prove this hypothesis, we first examined the expression levels of Rab18 in RSc and Huh7.5 cells. The expression levels of Rab18 were almost comparable between RSc cells and Huh7.5 cells at both the transcript (Fig. 2A) and protein levels (Fig. 2B). Two other members of the Ras-related small GTPases, Rab5 and Rab7, were also present at almost the same levels in RSc and Huh7.5 cells. We next examined the effect of the knockdown of Rab18 against HCV replication in RSc cells. The knockdown of Rab18 (Fig. 2C) had no effect on the RNA replication step (Fig. 2D). Rab18-knockdown Huh7.5 cells and genome-length HCV RNA-replicating O cells (Kato et al., 2009) also showed similar results (Fig. 2E and F, Supplemental Fig. S1A and B). However, we found that the knockdown of Rab18 caused a significant decrease in viral productivity in both RSc and Huh7.5 cells (Fig. 2G). In addition, the knockdown of ADRP (Supplemental Fig. S2A) also decreased viral productivity rather than HCV RNA replication (Supplemental Fig. S2B). Furthermore, we demonstrated that the overexpression of Rab18 (Fig. 2H) recovered the viral productivity (Fig. 2I) rather than viral RNA replication (Fig. 2J). From these results, we conclude that Rab18 is required for viral production of HCV.

Rab18 is required for viral assembly through the trafficking of the HCV-JFH-1 core protein to LDs

To clarify whether Rab18 is required for the viral assembly step, we first examined the localization of Rab18 and the HCV core protein in HCV-JFH-1-infected cells. The results revealed that Rab18

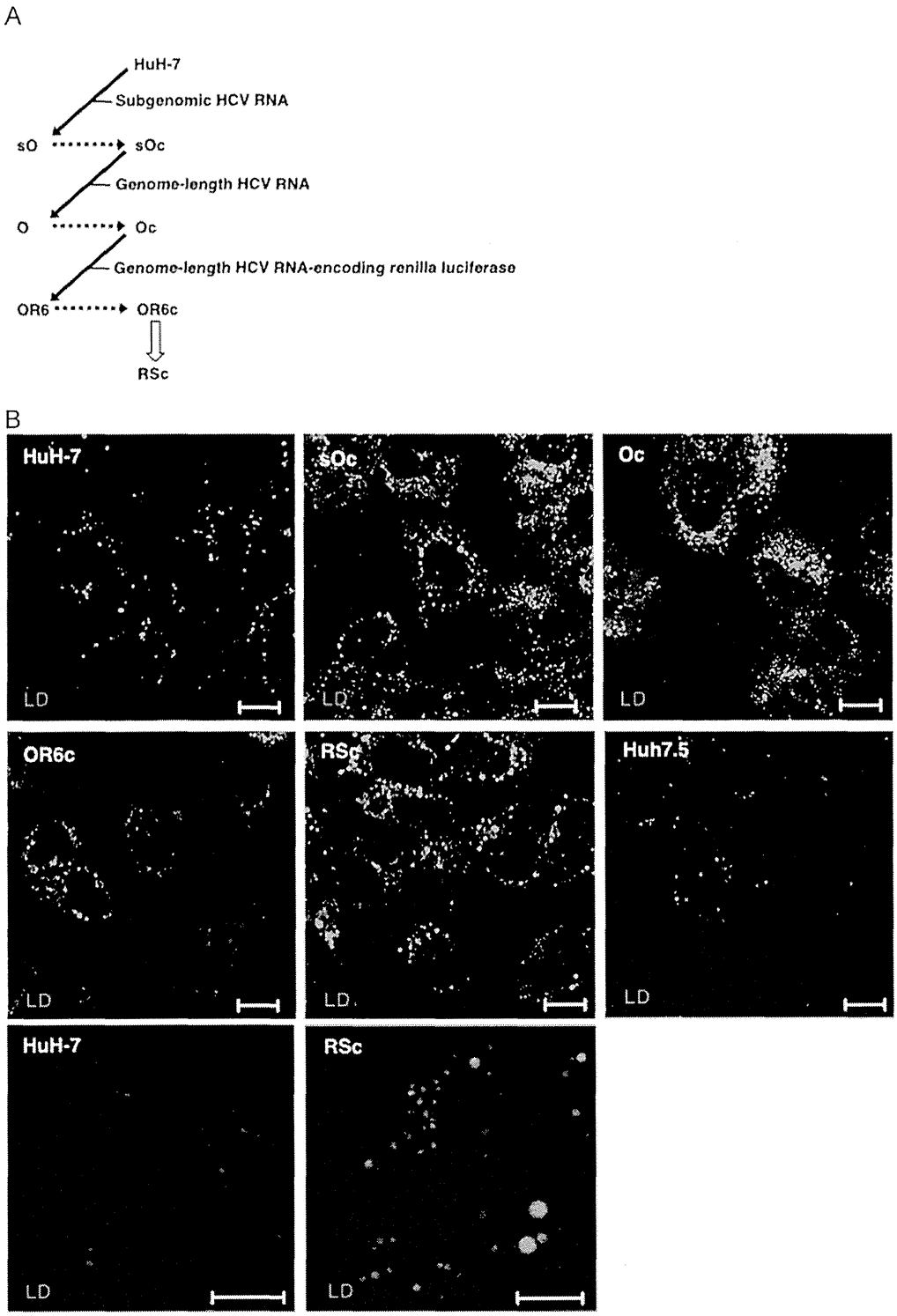

Fig. 1. RSc cells possess higher viral productivity in response to the infection with HCV-JFH-1 than Huh7.5 cells. (A) Outline for the establishment of our HCV RNA-replicating cells and their "cured" cells. Our HCV RNA-replicating cells (sO, O, and OR6 cells) are independently established by the transfection of HCV RNA into HuH-7 or cured cells (sOc or Oc cells) as previously reported (Ikeda et al., 2005, 2006; Kato et al., 2003). To prepare the cured cells, HCV RNA was eliminated from HCV RNA-replicating cells by the interferon treatment. RSc cells are one of the sublines of OR6c cells. The arrows with solid and dashed lines show the transfection of HCV RNA and the interferon treatment, respectively. (B) Visualization of LD under a confocal microscope. The panels show the fluorescence of LD by staining with BODIPY493/503. Bars, 20 μm. (C) Measurement of the mean fluorescence intensity of BODIPY493/503-stained cells by a flow cytometer. These levels were calculated relative to the level in HuH-7 cells, which was set at 1. (D) Quantitative RT-PCR analysis of HCV RNA in our cured cells 72 h after infection with HCV-JFH-1. Total RNA extracted from the cells was subjected to quantitative RT-PCR analysis. The experiments were performed in at least triplicate. (E) Time-course analysis of HCV RNA in RSc and Huh7.5 cells after infection with HCV-JFH-1. Total RNA was extracted from HCV-JFH-1-infected cells at each time point. (F) Quantitative RT-PCR analysis of HCV RNA in Huh7.5 cells 72 h after infection with intracellular (left panel) and extracellular (right panel) HCV-JFH-1. As intracellular or extracellular HCV-JFH-1, the lysate or the supernatant was recovered from RSc cells (designated J-RSc in the figure) and Huh7.5 cells (designated J-Huh7.5) 24 h after infection with HCV-JFH-1.

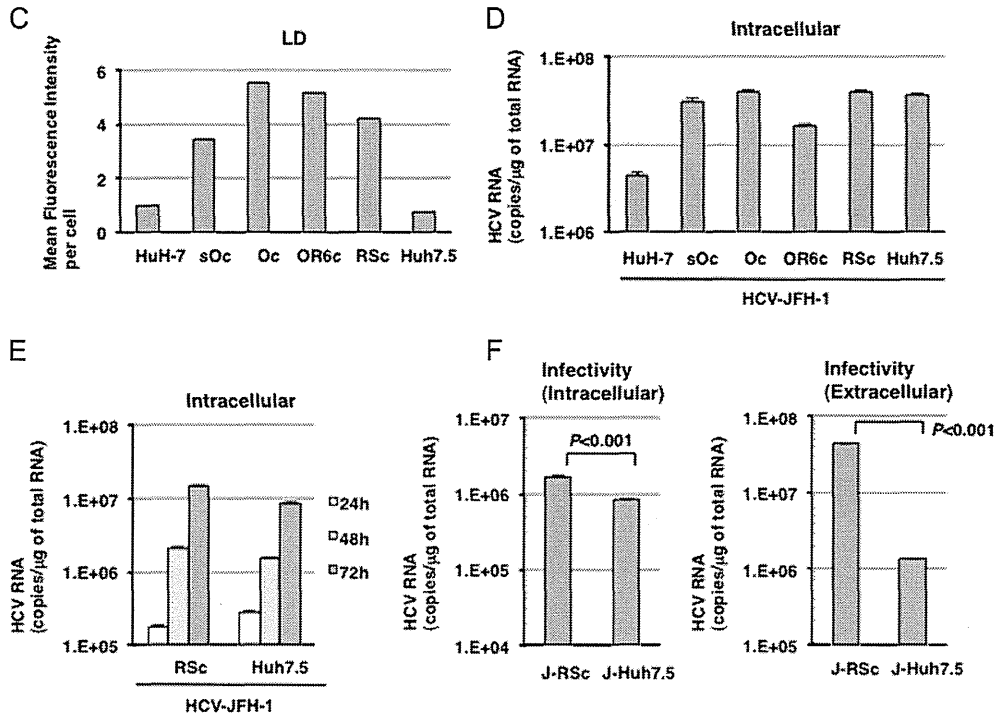

Fig. 1. (*continued*)

was co-localized with the core protein in HCV-JFH-1-infected RSc and Huh7.5 cells (Fig. 3A). We previously reported that the core protein was not recruited to LDs in O cells, from which no infectious virus was produced (data not shown). In fact, in contrast to HCV-JFH-1-infected RSc and Huh7.5 cells, co-localization of Rab18 and the core protein was not observed in O cells (Fig. 3B), although the expression of Rab18 were almost comparable levels among these cell lines (Supplemental Fig. S1C). We next examined the infectivity of intracellular viral particles in HCV-JFH-1-infected RSc siRab18 cells. The results revealed that the knockdown of Rab18 inhibited 90% of the production of intracellular viral particles (Fig. 3C) and the recruitment of the core protein to LDs (Fig. 3D). However, the knockdown of Rab4 (early endosome marker), other Ras-related small GTPase family member, inhibited only 40% of the production of intracellular viral particles (Supplemental Fig. S3C). These results suggest that Rab18 is particularly required for viral assembly through the trafficking of the core protein to LDs. Rab18 may be involved in the maturation of viral particles through membrane trafficking of the core protein from the ER to LDs.

Discussion

Previous proteomics analysis showed that a number of host factors were associated with LDs (Brasaemle et al., 2004). These LD-associated proteins may be required for the life cycle of HCV as well as the metabolism of lipids. During viral production, the HCV core protein is recruited to LDs in HCV-JFH-1-infected cells (Miyanari et al., 2007). In the present study, we suggest that one of the LD-associated proteins, Rab18, is required for trafficking of the HCV core protein to LDs and subsequent viral assembly.

The HCV core protein consists of three domains (domains 1, 2, and 3). Domain 2 (aa 118–173) contains two proline residues at aa positions 138 and 143, and a YATG sequence ranging from aa positions 164–167 that is essential for the association with LDs (Hope et al., 2002). These are conserved in both the JFH-1 strain (genotype 2a) and O strain (genotype 1b). However, the core protein was associated with LDs in HCV-JFH-1-infected RSc cells (Fig. 3D), but not in genome-length HCV RNA-replicating O cells (Kato et al., 2009). Matto et al. found that there were two morphologically distinct populations of the core protein (the ring-like and the dot-like pattern) in genome-length HCV RNA (genotype 1b)-replicating cells (Matto et al., 2004). The ring-like core protein was associated with LDs, and the dot-like core protein was associated with the detergent-resistant membranes and the lipid rafts essential for viral replication (Matto et al., 2004). We previously demonstrated that the core protein of the O strain showed a dot-like pattern (Kato et al., 2009), and that infectious virus was not produced from O cells (data not shown). In contrast to the core protein of the JFH-1 strain, the core protein of the O strain was not trafficked to LDs, and may have remained at the detergent-resistant membranes and the lipid rafts.

We also demonstrated that the core protein was co-localized with Rab18 in HCV-JFH-1-infected RSc cells, but not in O cells (Fig. 3B). In addition, we demonstrated that the knockdown of Rab18 did not inhibit HCV RNA replication in O cells as well as HCV-JFH-1-infected RSc cells (Supplemental Figs. S1B and S3B). However, in contrast to our results, Salloum et al. have previously observed that the knockdown of Rab18 inhibited HCV RNA replication in OR6 cells (Salloum et al., 2013). From these results, we speculate the clonality of HuH-7 cells as one of causes of this discrepancy. On the other hand, it also remains the possibility that the induction of IFN-β by shRNA reduced HCV RNA replication. Kenworthy et al. has previously reported that the introduction of shRNA by lentiviral vector may induce IFN-β (Kenworthy et al., 2009). Rab18 knockdown cells in the Salloum's paper were generated by the introduction of shRNA using lentiviral vector. In addition, Rab18 overexpression did not enhance HCV RNA replication in OR6 cells (Salloum et al., 2013). Another proteomic analysis suggested that Rab18 is upregulated in the lipid raft fraction of

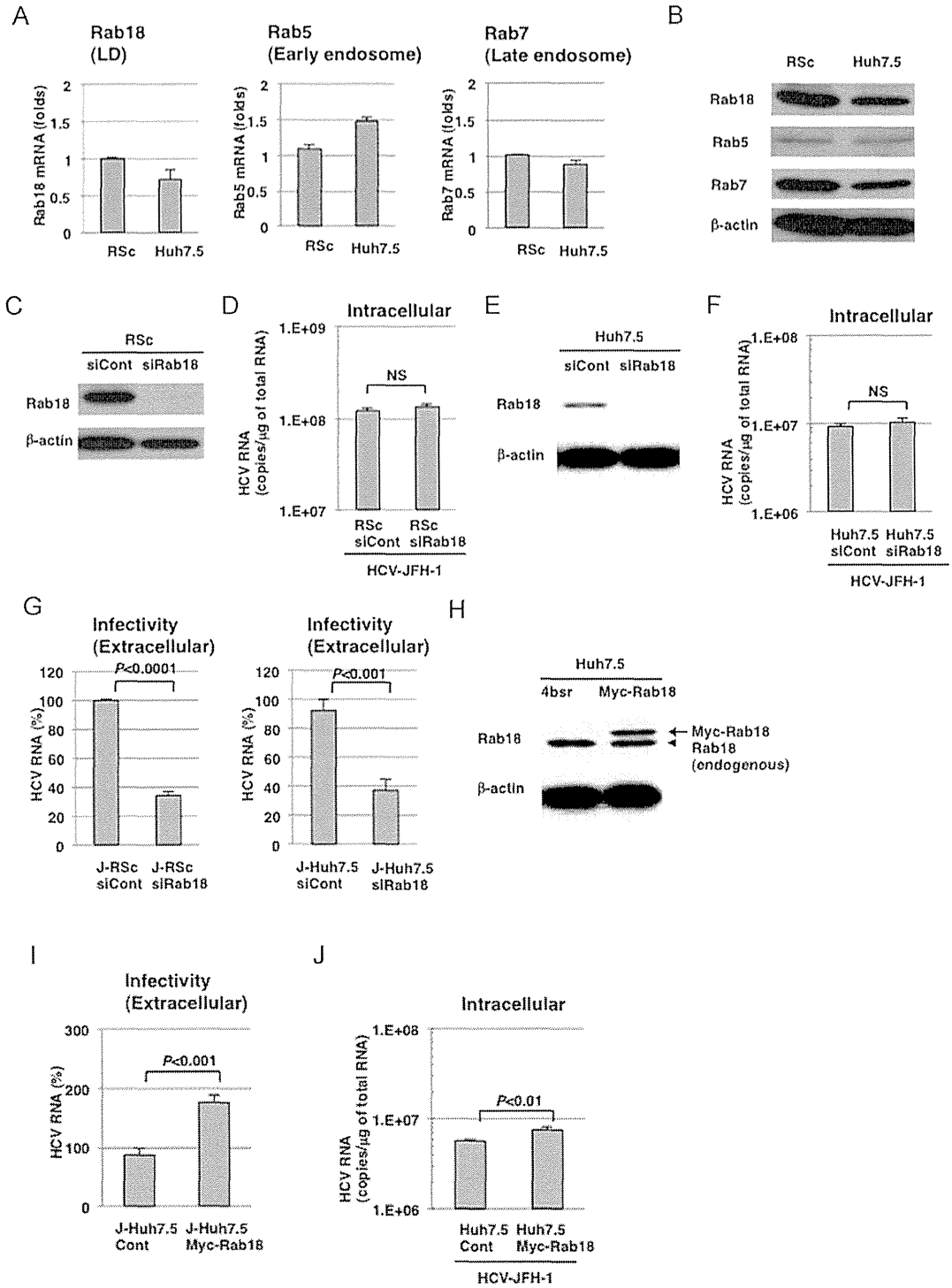

Fig. 2. Rab18 is required for viral production, but not viral RNA replication. (A) Quantitative RT-PCR analysis of Rab18, Rab5, and Rab7 mRNA in RSc and Huh7.5 cells. These levels were calculated relative to the level in RSc cells, which was set at 1. (B) Western blot analysis of Rab18, Rab5, and Rab7 in RSc and Huh7.5 cells. β-actin was included as a loading control. (C) Western blot analysis of Rab18 expression in RSc cells transfected with Rab18-specific (designated RSc siRab18 in the figure) or control (designated RSc siCont) siRNA. Cell lysates were prepared from RSc cells 120 h after transfection with Rab18-specific or control siRNA. (D) Quantitative RT-PCR analysis of HCV RNA in RSc siRab18 cells 24 h after infection with HCV-JFH-1. Transfection was performed 96 h before infection with HCV-JFH-1. NS: no significance. (E) Western blot analysis of Rab18 expression in Huh7.5 cells transfected with Rab18-specific (designated Huh7.5 siRab18) or control (designated Huh7.5 siCont) siRNA. (F) Quantitative RT-PCR analysis of HCV RNA in Huh7.5 siRab18 and siCont cells 24 h after infection with HCV-JFH-1. (G) Quantitative RT-PCR analysis of HCV RNA in Huh7.5 cells 72 h after infection with extracellular HCV-JFH-1. (Left panel) As extracellular HCV-JFH-1, the supernatant was recovered from RSc siCont cells (designated J-RSc siCont) or RSc siRab18 cells (designated J-RSc siRab18) 24 h after infection with HCV-JFH-1. (Right panel) The supernatant was also recovered from Huh7.5 siRab18 cells (designated J-Huh7.5 siRab18) and Huh7.5 siCont cells (designated J-Huh7.5 siCont) 24 h after infection with HCV-JFH-1. (H) Western blot analysis of Rab18 expression in Huh7.5 cells stably expressing Myc-tagged Rab18 (designated Huh7.5 Myc-Rab18). The arrow and arrowhead indicate exogenous (Myc-tagged) and endogenous Rab18, respectively. (I) Quantitative RT-PCR analysis of HCV RNA in Huh7.5 cells 72 h after infection with extracellular HCV-JFH-1. As extracellular HCV-JFH-1, the supernatant was recovered from Huh7.5 Cont (designated J-Huh7.5 Cont) or Huh7.5 Myc-Rab18 (designated J-Huh7.5 Myc-Rab18) 24 h after infection with HCV-JFH-1. (J) Quantitative RT-PCR analysis of HCV RNA in Huh7.5 Myc-Rab18 cells 24 h after infection with HCV-JFH-1.

genome-length HCV RNA (genotype 1b)-replicating cells (Mannova et al., 2006). These results may suggest that Rab18 also remained at the detergent-resistant membranes and the lipid rafts in the genome-length HCV RNA (genotype 1b)-replicating cells such as O cells. In addition, the gene silencing of Rab18 (Rab18-knockdown JFH-1-infected RSc cells) blocked localization of the HCV-JFH-1 core protein to LDs (Fig. 3D). Interestingly, the morphology of the population of HCV-JFH-1 core proteins was changed from a ring-like pattern to a dot-like pattern by the gene silencing of Rab18 (Fig. 3D). The HCV replication complex is formed on detergent-resistant membranes of the ER lumen (Shi et al., 2003). The ectopic expression of Rab18 induces the close apposition of LD to ER membranes through the reduction of ADRP (Ozeki et al., 2005). Rab18 may be one of the key host factors for the switch from the viral replication step to the viral assembly step through the close apposition of the detergent-resistant membranes to LDs. Rab18 may be an important target for the development of more effective anti-HCV reagents.

Materials and methods

Cell culture, reagents, and plasmids

Human hepatoma Huh7.5 cells were provided by Apath LLC (Brooklyn, NY). Huh7.5 cells, HuH-7 cells, and our established HuH-7-derived cells (sOC, Oc, OR6c, and RSc cells) were cultured in Dulbecco's modified Eagle's medium (Invitrogen, Carlsbad, CA) supplemented with 10% fetal bovine serum. Blasticidin (2 μg/ml) was used for the selection of Huh7.5 cells exogenously expressing Myc-Rab18. G418 (0.3 mg/ml) was also used for the selection of genome-length HCV RNA-replicating O cells.

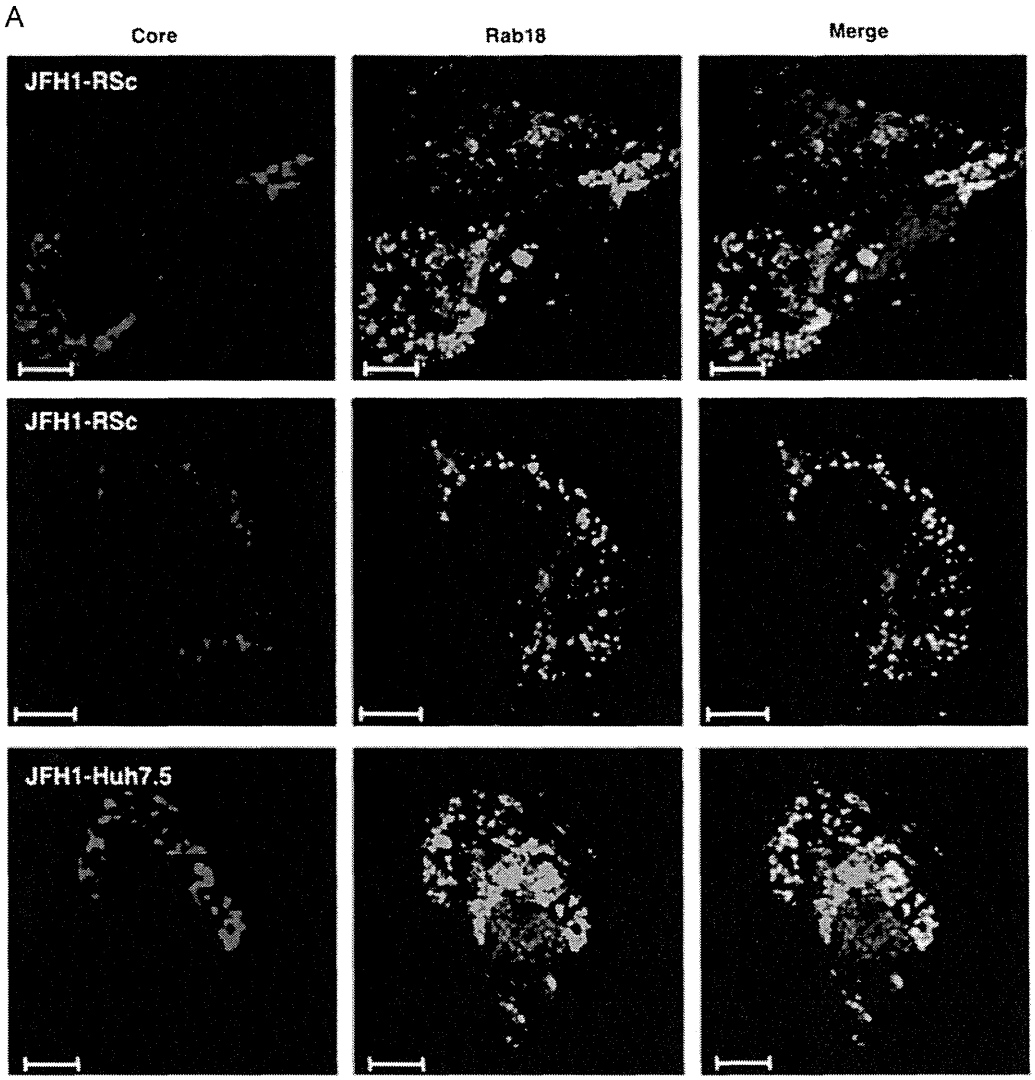

Fig. 3. Rab18 is required for viral assembly through the trafficking of HCV-JFH-1 core protein on LDs. (A) Visualization of the HCV-JFH-1 core protein (red) and Rab18 (green) under a confocal microscope. The panels show RSc or Huh7.5 cells 72 h after infection with HCV-JFH-1. Bars, 10 μm. (B) Visualization of the core protein (red) and Rab18 (green) in O cells. Bars, 10 μm. (C) Quantitative RT-PCR analysis of HCV RNA in Huh7.5 cells 72 h after infection with intracellular HCV-JFH-1. As intracellular HCV-JFH-1, the lysate was prepared from RSc siRab18 cells (designated J-RSc siRab18) and RSc siCont cells (designated J-RSc siCont) 24 h after infection with HCV-JFH-1. (D) Visualization of the HCV-JFH-1 core protein (red) and LD (green) under a confocal microscope. The panels show RSc siRab18 and siCont cells 72 h after infection with HCV-JFH-1. Bars, 10 μm.

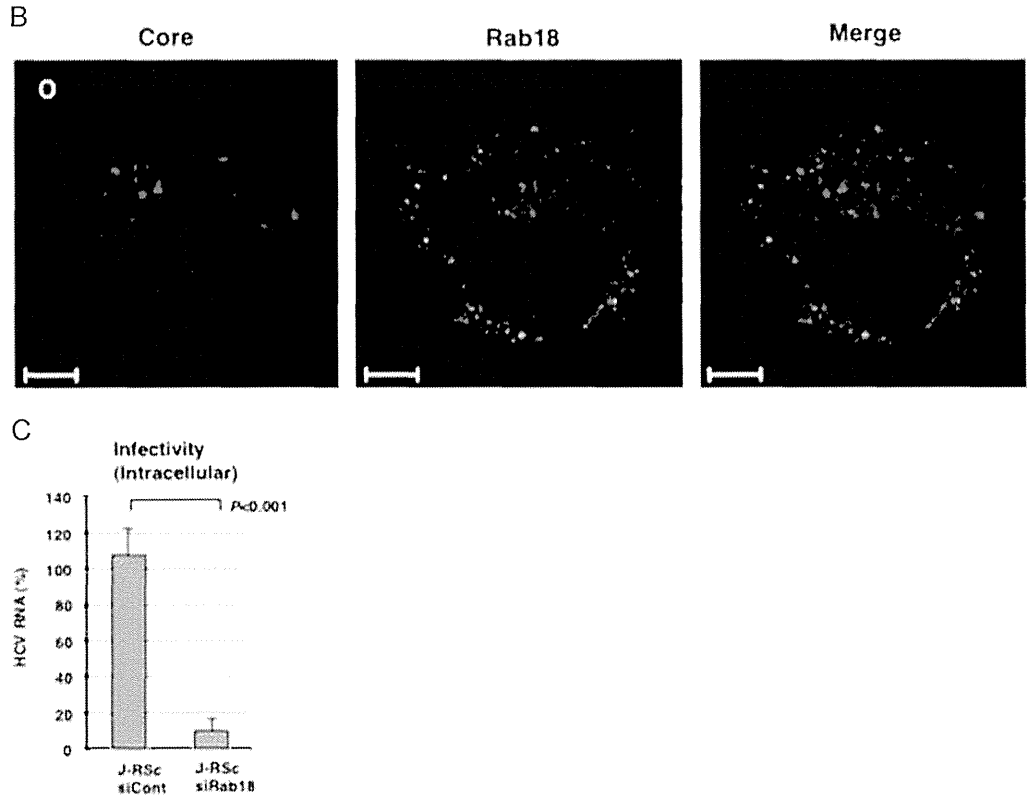

Fig. 3. (*continued*)

Immunofluorescence analysis

The LDs were stained with BODIPY493/503 (Invitrogen), and then photographed under a confocal microscope. Anti-Core antibody (CP11; Institute of Immunology, Tokyo, Japan) and anti-Rab18 antibody (Sigma, St. Louis, MO) were used as the primary antibodies. AlexaFluor 488-conjugated goat anti-rabbit antibody and AlexaFluor 594-conjugated goat anti-mouse antibody (Invitrogen) were used as the secondary antibodies. The intracellular localizations of HCV core protein and Rab18 were visualized and photographed under a confocal microscope as previously reported (Dansako et al., 2008). 4′-6-diamino-2-phenylindole (DAPI; Sigma) was used for visualization of the nucleus.

Flow cytometric analysis

The LDs were stained with BODIPY493/503 and then their mean fluorescence intensity was measured by a flow cytometer. The levels of LDs were calculated relative to the level in HuH-7 cells, which was set at 1.

Infection with HCV-JFH-1

The cells were infected with HCV-JFH1 (genotype 2a) for the appropriate time at a multiplicity of infection (MOI) of 1, and then the samples were prepared for the Western blot analysis, immunofluorescence analysis, and quantitative reverse transcription (RT)-PCR. Cell lysates and supernatants were prepared from the HCV-JFH-1-infected cells to monitor intracellular and extracellular infectivity. Intracellular HCV-JFH-1 was prepared from HCV-JFH-1-infected cells by repeated freeze-thaw cycles.

Generation of Rab18-knockdown cells

Small interfering RNAs (siRNAs) targeting Rab18 (Thermo Scientific; M-010824-00-0005) were prepared to generate Rab18-knockdown cells. siRNAs targeting Rab18 or non-targeting siRNAs (Thermo Scientific; D-001206-13-20) were introduced into RSc or Huh7.5 cells by DharmaFECT transfection reagent (Thermo Fisher Scientific, Waltham, MA). After transfection for the appropriate amount of time, Rab18-knockdown cells were infected with HCV-JFH-1.

Quantitative RT-PCR analysis

Total cellular RNA was isolated from HCV-JFH-1-infected cells by using an RNeasy mini kit (Qiagen, Hilden, Germany). RT was performed as previously described (Dansako et al., 2009). A SYBR Premix Ex Taq kit (TaKaRa Bio, Otsu, Japan) was used to measure the RNA levels of Rab18, Rab5, Rab7, GAPDH, or HCV. We used the following forward and reverse primer sets for quantitative PCR: for Rab18, 5′-GCGGAACGGGGTCAGGATGG-3′ (forward) and 5′-AAGAG CAGGCTGGACTTGCCC-3′ (reverse); for Rab5, 5′-GCTTGCTGCGGTCT CAGGTTTCT-3′ (forward) and 5′-TGGCCCGTTGGGTCTTGTTGC-3′ (reverse); for Rab7, 5′-CTCATCCAGGCCAGTCCCCGA-3′ (forward) and 5′–CCCGCTTTGTGGCCACTTGTC-3′ (reverse); for HCV and GAPDH, the primer sets are given in Dansako et al., 2013 and Dansako et al., 2003, respectively. The levels of Rab18, Rab5, Rab7, and HCV were normalized to the levels of GAPDH mRNA. The mRNA levels of Rab18, Rab5, and Rab7 in Huh7.5 cells were calculated relative to the level in RSc cells, which was set at 1. In vitro-transcribed HCV-JFH-1 RNA was used as the standard to calculate the amount of HCV RNA in HCV-JFH-1-infected cells. Data are the means ± SD from three independent experiments.

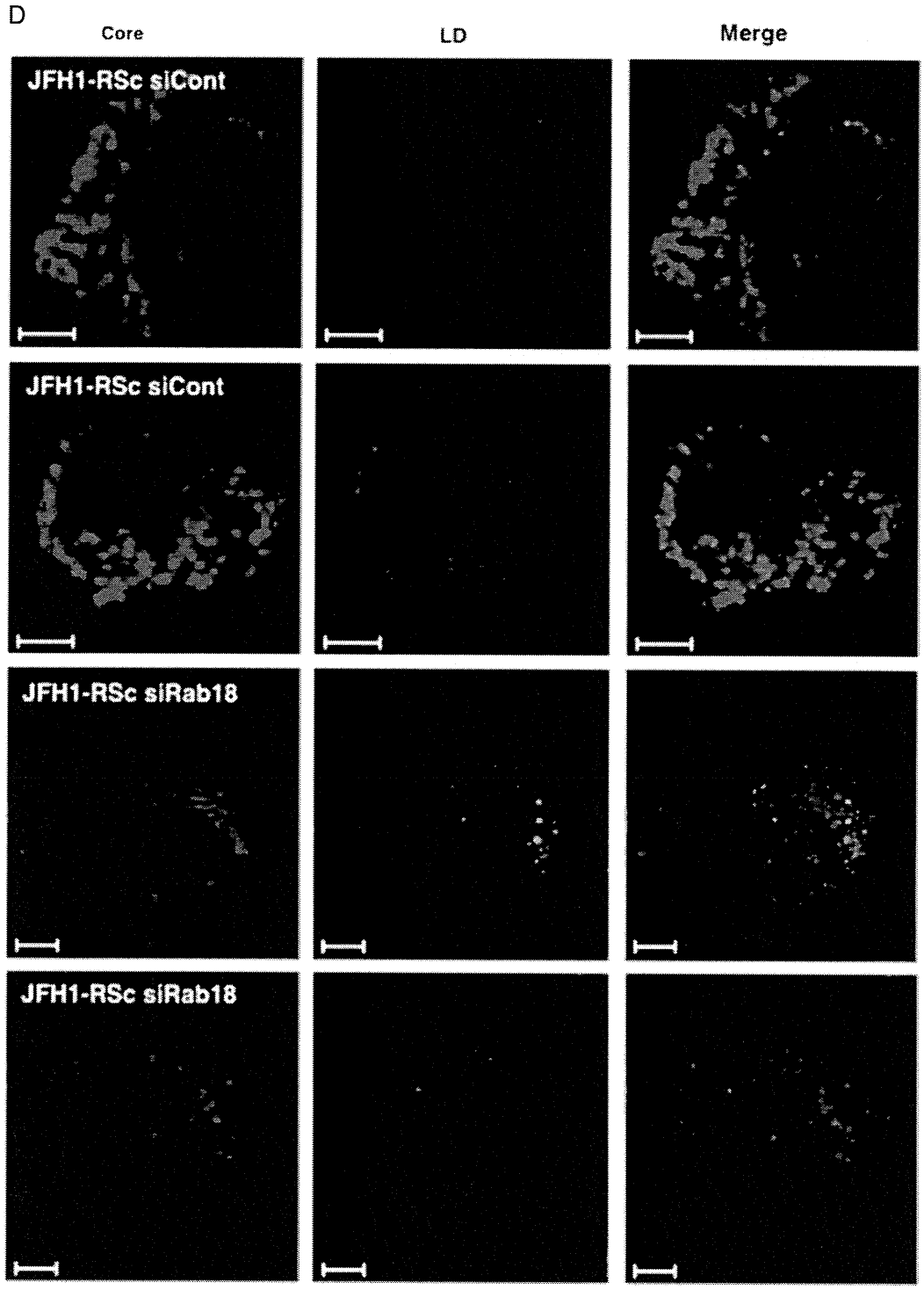

Fig. 3. (*continued*)

Western blot analysis

Preparation of cell lysates, and SDS-polyacrylamide gel electrophoresis were performed as previously described (Dansako et al., 2005). Gel was transferred to an Immobilon PVDF membrane (Millipore, Billerica, MA) by using a semi-dry transfer system: Horize BLOT 2MR (ATTO, Tokyo, Japan). Anti-Core (CP11; Institute of Immunology Co.), anti-Myc (PL14; Medical & Biological Laboratories, Nagoya, Japan), anti-Rab18 (Sigma), anti-Rab5 (S-19; Santa Cruz Biotechnology. Santa Cruz, CA), anti-Rab7 (Sigma),

and anti-β-actin antibody (AC-15; Sigma) were used in this study as primary antibodies. HRP-conjugated anti-mouse-IgG or anti-rabbit-IgG was used in this study as a secondary antibody (Cell Signaling Technology, Beverly, MA). Immunocomplexes were detected as previously described (Dansako et al., 2007).

Statistical analysis

Determination of the significance of differences among groups was assessed using the Student's *t*-test. $P < 0.05$ was considered statistically significant.

Acknowledgments

We thank Marie Iwado, Yoshiko Ueeda, Narumi Yamane and Takashi Nakamura for their technical assistance. We also thank Dr. Shinya Satoh for his helpful suggestions. This work was supported by Grants-in-Aid for Research on Hepatitis from the Ministry of Health, Labor, and Welfare of Japan; and by Japan Society for the Promotion of Science (JSPS) KAKENHI Grant no. 25293110.

Appendix A. Supplementary information

Supplementary data associated with this article can be found in the online version at http://dx.doi.org/10.1016/j.virol.2014.05.017.

References

Abe, K., Ikeda, M., Dansako, H., Naka, K., Kato, N., 2007. Cell culture-adaptive NS3 mutations required for the robust replication of genome-length hepatitis C virus RNA. Virus Res. 125, 88–97.

Ariumi, Y., Kuroki, M., Abe, K., Dansako, H., Ikeda, M., Wakita, T., Kato, N., 2007. DDX3 DEAD-box RNA helicase is required for hepatitis C virus RNA replication. J. Virol. 81, 13922–13926.

Ariumi, Y., Kuroki, M., Dansako, H., Abe, K., Ikeda, M., Wakita, T., Kato, N., 2008. The DNA damage sensors ataxia-telangiectasia mutated kinase and checkpoint kinase 2 are required for hepatitis C virus RNA replication. J. Virol. 82, 9639–9646.

Blight, K.J., McKeating, J.A., Rice, C.M., 2002. Highly permissive cell lines for subgenomic and genomic hepatitis C virus RNA replication. J. Virol. 76, 13001–13014.

Boulant, S., Douglas, M.W., Moody, L., Budkowska, A., Targett-Adams, P., McLauchlan, J., 2008. Hepatitis C virus core protein induces lipid droplet redistribution in a microtubule- and dynein-dependent manner. Traffic 9, 1268–1282.

Brasaemle, D.L., Dolios, G., Shapiro, L., Wang, R., 2004. Proteomic analysis of proteins associated with lipid droplets of basal and lipolytically stimulated 3T3-L1 adipocytes. J. Biol. Chem. 279, 46835–46842.

Choo, Q.L., Kuo, G., Weiner, A.J., Overby, L.R., Bradley, D.W., Houghton, M., 1989. Isolation of a cDNA clone derived from a blood-borne non-A, non-B viral-hepatitis genome. Science 244, 359–362.

Counihan, N.A., Rawlinson, S.M., Lindenbach, B.D., 2011. Trafficking of hepatitis C virus core protein during virus particle assembly. PLoS Pathog. 7, e1002302.

Dansako, H., Ikeda, M., Abe, K., Mori, K., Takemoto, K., Ariumi, Y., Kato, N., 2008. A new living cell-based assay system for monitoring genome-length hepatitis C virus RNA replication. Virus Res. 137, 72–79.

Dansako, H., Ikeda, M., Ariumi, Y., Wakita, T., Kato, N., 2009. Double-stranded RNA-induced interferon-beta and inflammatory cytokine production modulated by hepatitis C virus serine proteases derived from patients with hepatic diseases. Arch. Virol. 154, 801–810.

Dansako, H., Ikeda, M., Kato, N., 2007. Limited suppression of the interferon-beta production by hepatitis C virus serine protease in cultured human hepatocytes. FEBS J. 274, 4161–4176.

Dansako, H., Naganuma, A., Nakamura, T., Ikeda, F., Nozaki, A., Kato, N., 2003. Differential activation of interferon-inducible genes by hepatitis C virus core protein mediated by the interferon stimulated response element. Virus Res. 97, 17–30.

Dansako, H., Naka, K., Ikeda, M., Kato, N., 2005. Hepatitis C virus proteins exhibit conflicting effects on the interferon system in human hepatocyte cells. Biochem. Biophys. Res. Commun. 336, 458–468.

Dansako, H., Yamane, D., Welsch, C., McGivern, D.R., Hu, F.Y., Kato, N., Lemon, S.M., 2013. Class A scavenger receptor 1 (MSR1) restricts hepatitis C virus replication by mediating Toll-like receptor 3 recognition of viral RNAs produced in neighboring cells. PLoS Pathog. 9, e1003345.

Dejgaard, S.Y., Murshid, A., Erman, A., Kizilay, O., Verbich, D., Lodge, R., Dejgaard, K., Ly-Hartig, T.B., Pepperkok, R., Simpson, J.C., Presley, J.F., 2008. Rab18 and Rab43 have key roles in ER-Golgi trafficking. J. Cell Sci. 121, 2768–2781.

Hickenbottom, S.J., Kimmel, A.R., Londos, C., Hurley, J.H., 2004. Structure of a lipid droplet protein: the PAT family member TIP47. Structure 12, 1199–1207.

Hope, R.G., Murphy, D.J., McLauchlan, J., 2002. The domains required to direct core proteins of hepatitis C virus and GB virus-B to lipid droplets share common features with plant oleosin proteins. J. Biol. Chem. 277, 4261–4270.

Hutagalung, A.H., Novick, P.J., 2011. Role of Rab GTPases in membrane traffic and cell physiology. Physiol. Rev. 91, 119–149.

Ikeda, M., Abe, K., Dansako, H., Nakamura, T., Naka, K., Kato, N., 2005. Efficient replication of a full-length hepatitis C virus genome, strain O, in cell culture, and development of a luciferase reporter system. Biochem. Biophys. Res. Commun. 329, 1350–1359.

Ikeda, M., Abe, K., Yamada, M., Dansako, H., Naka, K., Kato, N., 2006. Different anti-HCV profiles of statins and their potential for combination therapy with interferon. Hepatology 44, 117–125.

Kato, N., 2001. Molecular virology of hepatitis C virus. Acta Med. Okayama 55, 133–159.

Kato, N., Mori, K., Abe, K., Dansako, H., Kuroki, M., Ariumi, Y., Wakita, T., Ikeda, M., 2009. Efficient replication systems for hepatitis C virus using a new human hepatoma cell line. Virus Res. 146, 41–50.

Kato, N., Sugiyama, K., Namba, K., Dansako, H., Nakamura, T., Takami, M., Naka, K., Nozaki, A., Shimotohno, K., 2003. Establishment of a hepatitis C virus subgenomic replicon derived from human hepatocytes infected in vitro. Biochem. Biophys. Res. Commun. 306, 756–766.

Kenworthy, R., Lambert, D., Yang, F., Wang, N., Chen, Z., Zhu, Haizhen, Zhu, F., Liu, C., Li, K., Tang, H., 2009. Short-hairpin RNAs delivered by lentiviral vector transduction trigger RIG-I-mediated IFN activation. Nucleic Acids Res. 37, 6587–6599.

Mannova, P., Fang, R.H., Wang, H., Deng, B., McIntosh, M.W., Hanash, S.M., Beretta, L., 2006. Modification of host lipid raft proteome upon hepatitis C virus replication. Mol. Cell. Proteomics 5, 2319–2325.

Matto, M., Rice, C.M., Aroeti, B., Glenn, J.S., 2004. Hepatitis C virus core protein associates with detergent-resistant membranes distinct from classical plasma membrane rafts. J. Virol. 78, 12047–12053.

Miyanari, Y., Atsuzawa, K., Usuda, N., Watashi, K., Hishiki, T., Zayas, M., Bartenschlager, R., Wakita, T., Hijikata, M., Shimotohno, K., 2007. The lipid droplet is an important organelle for hepatitis C virus production. Nat. Cell Biol. 9, 1089–1097.

Ohkoshi, S., Kojima, H., Tawaraya, H., Miyajima, T., Kamimura, T., Asakura, H., Satoh, A., Hirose, S., Hijikata, M., Kato, N., Shimotohno, K., 1990. Prevalence of antibody against non-A, non-B hepatitis-virus in Japanese patients with hepatocellular-carcinoma. Jpn. J. Cancer Res. 81, 550–553.

Ohsaki, Y., Maeda, T., Maeda, M., Tauchi-Sato, K., Fujimoto, T., 2006. Recruitment of TIP47 to lipid droplets is controlled by the putative hydrophobic cleft. Biochem. Biophys. Res. Commun. 347, 279–287.

Ozeki, S., Cheng, J.L., Tauchi-Sato, K., Hatano, N., Taniguchi, H., Fujimoto, T., 2005. Rab18 localizes to lipid droplets and induces their close apposition to the endoplasmic reticulum-derived membrane. J. Cell Sci. 118, 2601–2611.

Salloum, S., Wang, H., Ferguson, C., Parton, R.G., Tai, A.W., 2013. Rab18 binds to hepatitis C virus NS5A and promotes interaction between sites of viral replication and lipid droplets. PLoS Pathog. 9, e1003513.

Shavinskaya, A., Boulant, S., Penin, F., McLauchlan, J., Bartenschlager, R., 2007. The lipid droplet binding domain of hepatitis C virus core protein is a major determinant for efficient virus assembly. J. Biol. Chem. 282, 37158–37169.

Shi, S.T., Lee, K.J., Aizaki, H., Hwang, S.B., Lai, M.M.C., 2003. Hepatitis C virus RNA replication occurs on a detergent-resistant membrane that cofractionates with caveolin-2. J. Virol. 77, 4160–4168.

Targett-Adams, P., Boulant, S., McLauchlan, J., 2008. Visualization of double-stranded RNA in cells supporting hepatitis C virus RNA replication. J. Virol. 82, 2182–2195.

Biochemical and Biophysical Research Communications 447 (2014) 341–345

Contents lists available at ScienceDirect

Biochemical and Biophysical Research Communications

journal homepage: www.elsevier.com/locate/ybbrc

Anti-HCV activity of the Chinese medicinal fungus *Cordyceps militaris*

Youki Ueda, Kyoko Mori, Shinya Satoh, Hiromichi Dansako, Masanori Ikeda, Nobuyuki Kato *

Department of Tumor Virology, Okayama University Graduate School of Medicine, Dentistry, and Pharmaceutical Sciences, 2-5-1 Shikata-cho, Okayama 700-8558, Japan

ARTICLE INFO

Article history:
Received 12 March 2014
Available online 12 April 2014

Keywords:
Hepatitis C virus
HCV RNA-replication system
Assay systems for anti-HCV activity
Cordyceps militaris
Cordycepin

ABSTRACT

Persistent hepatitis C virus (HCV) infection causes chronic liver diseases and is a global health problem. Although the sustained virologic response rate in the treatment of genotype 1 using new triple therapy (pegylated-interferon, ribavirin, and telaprevir/boceprevir) has been improved by more than 70%, several severe side effects such as skin rash/ageusia and advanced anemia have become a problem. Under these circumstances, a new type of anti-HCV oral drug with few side effects is needed. Our recently developed HCV drug assay systems, including the HuH-7 cell line-derived OR6 and AH1R, and the Li23 cell line-derived ORL8 and ORL11, allow genome-length HCV RNAs (several strains of genotype 1b) encoding renilla luciferase to replicate efficiently. Using these systems as anti-HCV candidates, we have identified numerous existing medicines that can be used against HCV with few side effects, such as statins and teprenon. To obtain additional anti-HCV candidates, we evaluated a number of oral health supplements, and found that the capsule but not the liquid form of *Cordyceps militaris* (CM) (*Ascomycotinanorth, North Chinese caterpillar fungus*), which is used as a Chinese herbal medicine, exhibited moderate anti-HCV activity. In combination with interferon-α or ribavirin, CM exhibited an additive inhibitory effect. Among the main components of CM, cordycepin, but not ergosterol, contributed to the anti-HCV activity of CM. In consideration of all these results, we suggest that CM would be useful as an oral anti-HCV agent in combination with interferon-α and/or ribavirin.

1. Introduction

Hepatitis C virus (HCV) infection frequently causes chronic hepatitis, which often leads to liver cirrhosis and hepatocellular carcinoma. Since approximately 170 million people are infected with HCV worldwide, HCV infection is a serious global health problem [1]. HCV is an enveloped virus with a positive single-stranded RNA of the *Flaviviridae* family. The HCV genome encodes a large polyprotein precursor of approximately 3000 amino acids, which is cleaved into 10 proteins in the following order: Core, envelope 1 (E1), E2, p7, non-structural 2 (NS2), NS3, NS4A, NS4B, NS5A, and NS5B [2,3].

Recently, a new therapy for hepatitis C (genotype 1) with a combination of pegylated-interferon (PEG-IFN), ribavirin (RBV), and telaprevir/boceprevir (inhibitor of HCV NS3-4A protease) has been started as a global standard therapy [4]. Although the sustained virological response (SVR) in this therapy has improved approximately 70–80% [5], this therapy has several problems, such as severe side effects (skin rash, ageusia, advanced anemia, etc.), emergence of resistant viruses, and high treatment cost [5,6].

Although cells derived from the human hepatoma cell line HuH-7 have been used as the preferred culture system for the study of HCV life cycles and for the development of anti-HCV drugs [7], we previously found a new human hepatoma cell line, Li23, that enables reproducibility of the HCV life cycle [8]. Using the Li23 cell line, we developed Li23-derived drug assay systems (ORL8 and ORL11) in which a genome-length HCV RNA (the O strain of genotype 1b derived from an HCV-positive healthy carrier) encoding renilla luciferase (RL) replicates efficiently [8], based on a method previously reported in the development of a HuH-7-derived drug assay system (OR6) [9]. Since we demonstrated that the gene expression profile of Li23 cells was distinct from that in HuH-7 cells [10], and that the anti-HCV targets in Li23-derived cells (ORL8 and ORL11) were distinct from those in HuH-7-derived cells (OR6 and AH1R, which was developed using the AH1 strain of genotype 1b) [11–14], we considered that we might find a new type of anti-HCV agent by conducting a search using these two kinds of cell-based HCV RNA-replication assay systems. Indeed, we recently found that the preclinical antimalarial drugs N-89 and N-251 [15,16] exhibited potent anti-HCV activities [17].

Here, we report the further discovery that an oral health supplement used as a Chinese herbal medicine, *Cordyceps militaris*

* Corresponding author. Fax: +81 86 235 7392.
E-mail address: nkato@md.okayama-u.ac.jp (N. Kato).

http://dx.doi.org/10.1016/j.bbrc.2014.03.150
0006-291X/